



Pseudospectra of the Orr-Sommerfeld Operator

Author(s): Satish C. Reddy, Peter J. Schmid and Dan S. Henningson

Source: *SIAM Journal on Applied Mathematics*, Feb., 1993, Vol. 53, No. 1 (Feb., 1993), pp. 15-47

Published by: Society for Industrial and Applied Mathematics

Stable URL: <https://www.jstor.org/stable/2102271>

JSTOR is a not-for-profit service that helps scholars, researchers, and students discover, use, and build upon a wide range of content in a trusted digital archive. We use information technology and tools to increase productivity and facilitate new forms of scholarship. For more information about JSTOR, please contact support@jstor.org.

Your use of the JSTOR archive indicates your acceptance of the Terms & Conditions of Use, available at <https://about.jstor.org/terms>



JSTOR

Society for Industrial and Applied Mathematics is collaborating with JSTOR to digitize, preserve and extend access to *SIAM Journal on Applied Mathematics*

PSEUDOSPECTRA OF THE ORR–SOMMERFELD OPERATOR*

SATISH C. REDDY[†], PETER J. SCHMID[‡], AND DAN S. HENNINGSON[§]

Abstract. This paper investigates the pseudospectra and the numerical range of the Orr–Sommerfeld operator for plane Poiseuille flow. A number $z \in \mathbb{C}$ is in the ϵ -pseudospectrum of a matrix or operator A if $\|(zI - A)^{-1}\| \geq \epsilon^{-1}$, or, equivalently, if z is in the spectrum of $A + E$ for some perturbation E satisfying $\|E\| \leq \epsilon$. The numerical range of A is the set of numbers of the form (Au, u) , where (\cdot, \cdot) is the inner product and u is a vector or function with $\|u\| = 1$.

The spectrum of the Orr–Sommerfeld operator consists of three branches. It is shown that the eigenvalues at the intersection of the branches are highly sensitive to perturbations and that the sensitivity increases dramatically with the Reynolds number. The associated eigenfunctions are nearly linearly dependent, even though they form a complete set.

To understand the high sensitivity of the eigenvalues, a model operator is considered, related to the Airy equation that also has highly sensitive eigenvalues. It is shown that the sensitivity of the eigenvalues can be related qualitatively to solutions of the Airy equation that satisfy boundary conditions to within an exponentially small factor.

As an application, the growth of initial perturbations is considered. The near-linear dependence of the eigenfunctions implies that there is potential for energy growth, even when all the eigenmodes decay exponentially. Necessary and sufficient conditions for no energy growth can be stated in terms of both the pseudospectra and the numerical range. Bounds on the growth can be obtained using the pseudospectra.

Key words. Orr–Sommerfeld operator, eigenvalues, sensitivity, pseudospectra, numerical range, Airy equation, Green’s function, growth

AMS(MOS) subject classifications. 76E05, 34B25

1. Introduction. The stability of parallel shear flows is a fundamental problem of fluid dynamics and has been studied extensively for more than a century. For a review, see, for example, Drazin and Reid [9].

The linearized equations governing the evolution of small perturbations of a mean flow were first derived independently by Orr and Sommerfeld at the beginning of the twentieth century. Let us consider plane Poiseuille flow between walls at $y = \pm 1$ and with velocity $U(y) = 1 - y^2$ in the streamwise x direction. All quantities are nondimensionalized by the centerline velocity and the channel half-height. Let us assume that the streamfunction for a small two-dimensional perturbation to this flow can be written as

$$(1.1) \quad \Psi(x, y, t) = \phi(y, t)e^{i\alpha x},$$

where $\alpha > 0$ is a real wavenumber. Linearizing the Navier–Stokes equations, eliminating the pressure, and using the above expression for the perturbation, we obtain the evolution equation

$$(1.2) \quad -\{D^2 - \alpha^2\} \frac{\partial \phi}{\partial t} = -i\alpha \{(i\alpha R)^{-1}(D^2 - \alpha^2)^2 - U(D^2 - \alpha^2) + D^2 U\} \phi$$

* Received by the editors August 21, 1991; accepted for publication (in revised form) April 7, 1992.

[†] Courant Institute of Mathematical Sciences, 251 Mercer Street, New York, New York 10012. This research was started while the author was at the Massachusetts Institute of Technology and supported in part by an Alfred P. Sloan Foundation Doctoral Dissertation Award and a National Science Foundation Presidential Young Investigator Award to L. N. Trefethen.

[‡] Department of Mathematics, Massachusetts Institute of Technology, Cambridge, Massachusetts 02139.

[§] Department of Mathematics, Massachusetts Institute of Technology, Cambridge, Massachusetts 02139. This research was supported in part by the Aeronautical Research Institute of Sweden.

with initial and boundary conditions $\phi(y, 0) = \phi_0(y)$, $\phi(\pm 1, t) = D\phi(\pm 1, t) = 0$, where $D = \partial/\partial y$ and R is the Reynolds number [29]. This equation can be written in the form

$$(1.3) \quad \frac{\partial \phi}{\partial t} = -i\alpha \mathcal{B}^{-1} \mathcal{A} \phi, \quad \phi(y, 0) = \phi_0(y), \quad \phi(\pm 1, t) = D\phi(\pm 1, t) = 0,$$

where $\mathcal{A} = (i\alpha R)^{-1} (D^2 - \alpha^2)^2 - U(D^2 - \alpha^2) + D^2 U$ and $\mathcal{B} = -(D^2 - \alpha^2)$. We call the operator defined by $\mathcal{S} = \mathcal{B}^{-1} \mathcal{A}$ the *Orr–Sommerfeld* (O–S) *operator* [8]. According to (1.3), the O–S operator maps a perturbation $\phi(y, t)$ to its derivative with respect to time.

A standard method for analyzing the initial boundary value problem (1.3) is to consider an expansion in terms of the eigenfunctions of the O–S operator. Let us suppose that ϕ can be written in the form

$$(1.4) \quad \phi(y, t) = \tilde{\phi}(y) e^{-i\alpha\lambda t}.$$

Substituting this expression into (1.2), we obtain the celebrated *Orr–Sommerfeld equation*

$$(1.5) \quad \mathcal{A}\tilde{\phi} = \lambda \mathcal{B}\tilde{\phi}, \quad \tilde{\phi}(\pm 1) = D\tilde{\phi}(\pm 1) = 0.$$

The O–S equation is a boundary value problem for the eigenvalue λ and the associated eigenfunction $\tilde{\phi}$. The eigenvalues and eigenfunctions of (1.5) are precisely the eigenvalues and eigenfunctions of the O–S operator \mathcal{S} [8].

Much of the work on the O–S equation has focused on determining its eigenvalues, particularly the least stable one [9]—that is, the eigenvalue with maximal imaginary part. If there is a solution to (1.5) with $\text{Im } \lambda > 0$, then the perturbation Ψ can grow exponentially in time. The mean flow in this case is said to be *linearly unstable*. Results for the least stable eigenvalue have been used to determine the *neutral stability curve*, defined as the boundary of the region in the α - R plane where the O–S equation has linearly unstable solutions. Theoretical work has shown that the O–S operator for a bounded domain has an infinite number of discrete eigenvalues and that the associated eigenfunctions form a complete set [8], [29].

The O–S operator is *nonnormal*; its eigenfunctions are not *orthogonal*. The behavior of a normal matrix or operator in many applications is completely determined by its eigenvalues. This need not be the case for nonnormal matrices and operators. The eigenvalues of a nonnormal operator may be highly sensitive to perturbations, and the eigenfunctions, though complete, may be nearly linearly dependent. In such cases, it may be inappropriate to analyze matrix or operator behavior by considering the eigenvalues alone.

An alternative method of analyzing the behavior of a nonnormal matrix or operator is to consider the *pseudospectra* [33]. Let A be a matrix and let $\|\cdot\|_2$ denote the discrete 2-norm. For any $\epsilon \geq 0$, a number $z \in \mathbb{C}$ lies in the ϵ -pseudospectrum, denoted by $\Lambda_\epsilon(A)$, if $\|(zI - A)^{-1}\|_2 \geq \epsilon^{-1}$. Equivalently, $z \in \Lambda_\epsilon(A)$ if z lies in the spectrum of $A + E$ for some matrix E satisfying $\|E\|_2 \leq \epsilon$. The sets $\Lambda_\epsilon(A)$ are nested, and $\Lambda_0(A) \equiv \Lambda(A)$ is the spectrum of A . If A is normal, then $\Lambda_\epsilon(A)$ is simply the union of the ϵ -balls centered at the eigenvalues. On the other hand, the ϵ -pseudospectrum of a nonnormal matrix or operator may be much larger than the spectrum, even if $\epsilon \ll 1$. These ideas extend in a straightforward manner to operators and more general norms.

The notion of the pseudospectrum was introduced by Trefethen to analyze the behavior of nonnormal matrices in numerical analysis [33]. It has been shown that the behavior of nonnormal matrices in many applications may be better understood by considering the pseudospectra instead of the eigenvalues alone [34]. One such application is the stability analysis of method of lines discretizations of partial differential equations [27]. Another is convergence analysis of iterative methods for linear systems [22], [33], where iteration parameters based on the pseudospectra can lead to faster convergence than parameters based on the spectrum. Studying the pseudospectra of a matrix or operator A is equivalent to studying the *resolvent* $(zI - A)^{-1}$, which plays a fundamental role in many areas of mathematical analysis [19].

Another set that is useful for analyzing matrix or operator behavior is the *numerical range* or *field of values* [16], [19]. The numerical range is a single set. It is related to the pseudospectra and contains the spectrum in its closure. For a matrix A , it is defined as the set of all numbers (Au, u) , where (\cdot, \cdot) is the inner product associated to the 2-norm and u is a vector with unit norm. For a normal matrix, the numerical range is simply the convex hull of the spectrum, but for a nonnormal matrix it may be much larger than the spectrum.

The purpose of this paper is to study the pseudospectra and the numerical range of the O–S operator. We employ both analytic and numerical techniques. Let us start with the numerical computation that first initiated our study of the Orr–Sommerfeld operator. We approximate the operator \mathcal{S} for plane Poiseuille flow with $R = 10,000$ and $\alpha = 1$ using a Chebyshev hybrid discretization [15]. Following the standard practice of considering the even eigenfunctions of the O–S equation, we restrict our attention to the *even part* of the O–S operator.¹ The discretization converts the O–S operator into a matrix \hat{S} . We compute the eigenvalues of \hat{S} using a routine from the linear algebra package Matlab. We approximate the ϵ -pseudospectrum for $\epsilon = 10^{-6}$ by computing the eigenvalues of 100 perturbed matrices $\hat{S} + E$, where E is a random complex matrix with $\|E\|_2 = 10^{-6}$.² The results of these computations are shown in Fig. 1.

The portion of the spectrum of \hat{S} shown in Fig. 1(a) has the familiar three-branch structure of the O–S spectrum for Poiseuille flow [21]. The eigenvalues of the perturbed matrices $\hat{S} + E$ exhibit several striking features. The eigenvalues near the intersection of the \mathbf{A} , \mathbf{P} , and \mathbf{S} branches are highly sensitive to perturbations. A perturbation of size 10^{-6} has changed these eigenvalues by $O(1)$. In contrast, the eigenvalues away from the intersection of the branches, particularly the least stable modes, are relatively insensitive to perturbations. If \hat{S} were normal, then the eigenvalues of the perturbed matrices $\hat{S} + E$ would lie within a distance 10^{-6} of the eigenvalues of \hat{S} .

We find that the results in Fig. 1(b) are essentially independent of the type of numerical discretization and the number of modes used, and that the sensitivity to perturbations grows dramatically with R . One implication of these results is that

¹ The even part of \mathcal{S} can be defined in the following manner. The domain of the O–S operator can be written as the direct sum $D(\mathcal{S}) = D_e \oplus D_o$, where D_e and D_o are the spaces of even and odd functions in $D(\mathcal{S})$, respectively. Similarly, the O–S operator can be written as the direct sum $\mathcal{S} = \mathcal{S}_e \oplus \mathcal{S}_o$. The *even part* \mathcal{S}_e has domain D_e and maps an even perturbation $\phi_e \in D_e$ to its derivative with respect to time (1.3).

² Each element of E is of the form $a + ib$, where initially a and b are independently drawn from a normal distribution with mean zero and standard deviation 1. Each element of the resulting matrix is then uniformly scaled so that its discrete 2-norm satisfies $\|E\|_2 = 10^{-6}$. All calculations in this paper are performed using double-precision arithmetic.

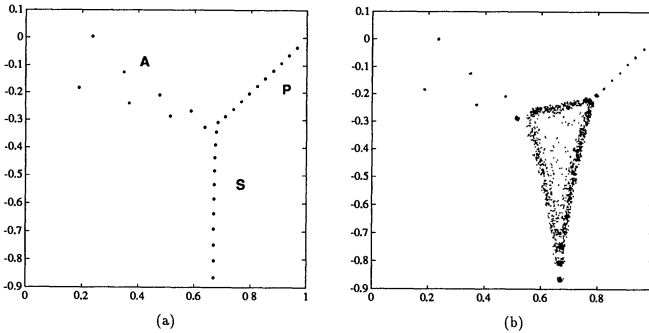


FIG. 1. Eigenvalues of \hat{S} and of $\hat{S} + E$ for Poiseuille flow with $R = 10,000$ and $\alpha = 1$. The asterisks in (a) are the 30 least stable eigenvalues of \hat{S} . The labels **A**, **P**, and **S** are the names introduced by Mack [21] for the three branches of eigenvalues. The dots in (b) are the 30 least stable eigenvalues of 100 perturbed matrices $\hat{S} + E$, where E is a random complex matrix with $\|E\|_2 = 10^{-6}$.

the computation of highly sensitive eigenvalues is significantly affected by rounding and discretization errors when the Reynolds number is large. A more fundamental implication is that the eigenfunctions associated with the eigenvalues near the intersection of the branches are nearly linearly dependent and that expansions using these eigenfunctions may be inappropriate at high Reynolds numbers.

To gain insight into the sensitivity of the eigenvalues at the intersection of the branches, we consider the differential operator

$$(1.6) \quad \mathcal{T} = -\frac{1}{i\alpha R} \frac{d^2}{dy^2} + y$$

with homogeneous boundary conditions at $y = \pm 1$. The associated eigenvalue problem can be written as

$$(1.7) \quad \frac{1}{i\alpha R} \frac{d^2\phi}{dy^2} - (y - \lambda)\phi = 0, \quad \phi(\pm 1) = 0,$$

and is related to the equation for the Squire modes for Couette flow [13]. Like the O-S operator \mathcal{S} , the model operator \mathcal{T} has a countable spectrum consisting of three branches. The eigenvalues at the intersection of the branches are highly sensitive to perturbations. The high sensitivity of the eigenvalues can be explained qualitatively. It is due to the existence of normalized solutions to the differential equation in (1.7) that satisfy the boundary conditions to within an exponentially small factor for values of λ near the intersection of the branches.

The nonnormality of the O-S operator has important consequences for the energy growth of initial perturbations. Orszag showed that, if $R \leq R_c \approx 5772$, then all the eigenvalues of the O-S operator for plane Poiseuille flow lie in the lower half-plane for all values of α [24]. Due to the nonorthogonality of the O-S eigenfunctions, however, the energy of a perturbation may increase even if R is less than this critical value. Using *energy methods*, Orr showed that there is no energy growth for two-dimensional perturbations if $R < R_g \approx 87.7$ [23]. In terms of the numerical range, *there is no energy growth if and only if the numerical range of \mathcal{S} lies in the closed lower half-plane*. This condition is one part of the Hille-Yosida theorem and is equivalent to conditions obtained using energy methods [18], [23]. Now, if $R_g < R < R_c$, then there is the potential for transient growth in the energy. This growth was first computed by Farrell

[10], and we show that growth by a factor as large as ≈ 51 may occur at subcritical Reynolds numbers. The transient growth depends on how far the pseudospectra extend into the upper half-plane.

The sensitivity of the O–S eigenvalues has been noted in previous numerical studies. Orszag computed the stable modes far below the real axis and noted that fewer significant digits could be obtained for the eigenvalues at the intersection of the branches than for the eigenvalues near the real axis [24]. This property was also noted by Herbert [15] and Mack [21]. In recent work, Farrell and Butler have noted the connection between nonorthogonality of the O–S eigenfunctions and growth and have computed the maximum transient growth for two- and three-dimensional perturbations to Poiseuille and Couette flows [4], [10]. Yudovich has done theoretical work on the resolvent of a linearized Navier–Stokes operator for a bounded three-dimensional domain and has applied these results to the analysis of growth [35].

This paper is organized as follows. Section 2 defines the pseudospectrum and the numerical range and discusses their properties. Section 3 describes the Hille–Yosida theorem and other results for bounding growth. Section 4 presents background material on the O–S operator and bounds on its numerical range. Section 5 presents numerical results on the pseudospectra of the O–S operator. Section 6 examines the pseudospectra of the model operator. Section 7 considers transient growth of initial perturbations.

Finally, we stress that this is not a paper about rounding errors or, for that matter, numerical methods for solving the O–S equation. Our goal is to understand the behavior of the O–S operator. We use analytic and numerical methods to achieve this end.

2. Definitions of the pseudospectrum and numerical range. We now present formal definitions of the pseudospectrum and the numerical range and describe their properties. This section contains results from an early draft of [32]. We have attempted to make it as complete as possible by citing secondary sources for the main results.

For simplicity, we begin with a definition for matrices. Let A be a square matrix of dimension N with spectrum $\Lambda(A)$ and resolvent set $\rho(A) = \mathbf{C} \setminus \Lambda(A)$. Let $\|\cdot\|$ be the norm generated by the inner product (\cdot, \cdot) . These terms are standard [19]. The definition of the ϵ -pseudospectrum can be put in the following form [28].

DEFINITION. Let $\epsilon \geq 0$ be given. A number z is in the ϵ -pseudospectrum of A , which we denote by $\Lambda_\epsilon(A)$, if any of the following equivalent conditions is satisfied:

- (i) z is an eigenvalue of $A + E$ for some perturbation matrix with $\|E\| \leq \epsilon$;
- (ii) There exists $u \in \mathbf{C}^N$ with $\|u\| = 1$ such that $\|Au - zu\| \leq \epsilon$;
- (iii) $z \in \rho(A)$ and $\|(zI - A)^{-1}\| \geq \epsilon^{-1}$ or $z \in \Lambda(A)$.

The proof of the equivalence of (i)–(iii) is straightforward.

Proof. We need only prove the equivalence of (i) and (ii), since the equivalence of (ii) and (iii) follows from the definition of the norm. First, assume that (i) holds and suppose that z is an eigenvalue of $A + E$ with the associated normalized eigenfunction u . Using the fact that $(A + E)u = zu$, it follows that $\|Au - zu\| = \|Eu\| \leq \|E\| \leq \epsilon$. Now assume that (ii) holds and suppose that $Au - zu = v$. For all $w \in \mathbf{C}^N$, we define the matrix E by $Ew = -v(u, w)$. Using the definition of the norm and (ii), it follows that $\|E\| = \|v\| \|u\| = \|v\| \leq \epsilon$. Since $Eu = -v$, it follows $(A + E)u = zu$. Hence, z is an eigenvalue of $A + E$. \square

The vector u in (ii) is called an ϵ -pseudo-eigenvector. The matrix $(zI - A)^{-1}$ is the resolvent. It is easy to see from the definition that the pseudospectra are nested

as follows: $\Lambda_{\epsilon'}(A) \subseteq \Lambda_\epsilon(A)$ if $\epsilon' \leq \epsilon$. In addition, $\Lambda_0(A) = \Lambda(A)$. A normal matrix has a complete set of eigenfunctions, which are orthogonal with respect to the inner product (\cdot, \cdot) . Its ϵ -pseudospectrum is simply the union of the closed balls of radius ϵ centered at the eigenvalues. The ϵ -pseudospectrum of a nonnormal matrix, however, may be much larger than the spectrum; see Theorem 2.1, below.

The definition can be generalized to infinite-dimensional operators. Let \mathcal{H} be a Hilbert space with inner product (\cdot, \cdot) and norm $\|\cdot\|$. Let $A : \mathcal{H} \rightarrow \mathcal{H}$ be a *closed* linear operator with spectrum $\Lambda(A)$, resolvent set $\rho(A)$, and a domain $D(A)$ that is dense in \mathcal{H} . The precise definition of a closed operator is not important for our purposes; see [19] for details. Most differential operators of interest in applications, including the O-S and model operators, can be defined to be closed.

We take (iii) to be the fundamental definition of the ϵ -pseudospectrum for closed linear operators. In general, conditions (i)–(iii) may not be equivalent for closed linear operators. Unlike the set defined by (iii), which is closed, the sets defined by (i) and (ii) may not contain their boundaries if A is an operator. These conditions can be made equivalent [32].

The above definition establishes a connection between the resolvent and the eigenvalues of perturbed operators. This connection plays a fundamental role in the perturbation theory for linear operators [19]. We stress that analysis based on pseudospectra is equivalent to analysis based on the resolvent. One of the principal advantages of pseudospectra is that they are visually appealing. In addition to being employed for theoretical purposes, they have also been used to develop an intuition about operator behavior [34]. For completeness, we state both the resolvent and the pseudospectral versions of relevant results in the discussion below.

It is straightforward, though computationally expensive, to estimate the pseudospectra of a matrix numerically. The boundaries of the pseudospectra are the level curves of the norm of the resolvent $\|(zI - A)^{-1}\|$. These boundaries can be determined by first computing $\|(zI - A)^{-1}\|$ for values of z on a grid in the complex plane and then sending this data to a contour plotter. Examples of this type of computation are presented in §5. The ϵ -pseudospectrum may be approximated more speedily and roughly, as in Fig. 1(b), by plotting the eigenvalues of $A + E$ for several perturbation matrices E with $\|E\| = \epsilon$.

It is more difficult to determine the ϵ -pseudospectrum of a matrix or operator analytically. The pseudospectra can be approximated by computing sets L_ϵ and U_ϵ such that $L_\epsilon \subseteq \Lambda_\epsilon \subseteq U_\epsilon$. These sets may be determined by bounding the resolvent.

A lower bound for the pseudospectra, valid for both matrices and closed linear operators, can be obtained by computing a lower bound for the norm of the resolvent. Suppose that there is a function $b(z)$ such that $\|(zI - A)^{-1}\| \geq b(z)$ for each $z \in \rho(A)$. Then

$$(2.1) \quad L_\epsilon(A) = \{z \in \rho(A) : b(z) \geq \epsilon^{-1}\} \cup \Lambda(A)$$

is a lower bound for the ϵ -pseudospectrum for all $\epsilon \geq 0$. A trivial lower bound follows from the inequality

$$(2.2) \quad \|(zI - A)^{-1}\| \geq \frac{1}{\text{dist}\{z, \Lambda(A)\}} \quad \forall z \in \rho(A),$$

where $\text{dist}\{z, \Lambda(A)\}$ is the distance of z to the spectrum of A [19]. A general method for obtaining lower bounds follows from the definition of the resolvent norm: If $z \in$

$\rho(A)$, then

$$(2.3) \quad \|(zI - A)^{-1}\| = \left[\inf_{u \in D(A), u \neq 0} \frac{\|Au - zu\|}{\|u\|} \right]^{-1}.$$

The function $b(z)$ can be determined by searching for trial elements $u_z \in D(A)$, scaled to have norm 1, so that the quantity in the brackets in (2.3) is as small as possible. If $b(z) = \|(A - zI)u_z\|^{-1}$, then $\|(zI - A)^{-1}\| \geq b(z)$.

An upper bound for the pseudospectra is obtained by determining an upper bound for the resolvent. Suppose that the function $B(z)$ satisfies $B(z) \geq \|(zI - A)^{-1}\|$ for each $z \in \rho(A)$. The set

$$(2.4) \quad U_\epsilon(A) = \{z \in \rho(A) : B(z) \geq \epsilon^{-1}\} \cup \Lambda(A)$$

is an upper bound for the ϵ -pseudospectrum for all $\epsilon \geq 0$. For differential operators, an upper bound can often be determined using the Green's function of the associated differential equation. The sharpness of these bounds depends on how close $B(z)$ and $b(z)$ are to $\|(zI - A)^{-1}\|$.

The degree of normality of a matrix or operator is related to the degree of linear independence of its eigenvectors. This last quantity can be measured. Let $\{\phi_j\}$ be a set of K linearly independent functions in \mathcal{H} , normalized so that $\|\phi_j\| = 1$. Let W denote the space spanned by these functions and suppose that the normalized elements $\{\psi_j\}$ form an orthogonal basis for W with respect to (\cdot, \cdot) . Any function $f \in W$ can be expressed in terms of either set of basis functions as follows:

$$(2.5) \quad f = \sum_{j=1}^K a_j \phi_j = \sum_{j=1}^K b_j \psi_j.$$

The two sets of expansion coefficients can be related. If a and b are the K -vectors of the coefficients, then $b = U_W a$, where U_W is a square matrix of dimension K . The *condition number* of the basis $\{\phi_j\}$ is defined by

$$(2.6) \quad \kappa = \|U_W\|_2 \|U_W^{-1}\|_2,$$

where the subscript 2 denotes the 2-norm. The condition number satisfies $\kappa \geq 1$ and $\kappa = 1$ if and only if the original functions $\{\phi_j\}$ are orthonormal. Using this last fact, it can be shown that κ depends only on the original basis $\{\phi_j\}$ and not on the choice of the orthonormal basis. The number κ gives an approximate upper bound for the magnitude of the coefficients $\{a_j\}$ in the expansion of a function with norm 1. When κ is large, the functions $\{\phi_j\}$ are a poor basis for W . An orthonormal basis for W and the corresponding matrix U_W can be computed from the functions $\{\phi_j\}$ using the Gram–Schmidt procedure [11]; see Appendix B.

The condition number can be related to the pseudospectra. To do this, we must first project the closed linear operator A onto a finite-dimensional space. Suppose that $\{\phi_j\}$ is a set of K linearly independent normalized eigenfunctions of A and that $\{\lambda_j\}$ are the associated eigenvalues. We project A onto the space W spanned by the eigenfunctions. The resulting operator, which we denote by A_W , maps functions from W to W . For each ϕ_j , we have $A_W \phi_j = \lambda_j \phi_j$. The formula for $A_W f$ for arbitrary $f \in W$ can be determined using (2.5). The spectrum of A_W is $\{\lambda_j\}$. Bounds on the pseudospectra are given by the following result [32]. Here Δ_ϵ is the closed disk of

radius ϵ centered at the origin and the sum of sets is defined by $U_1 + U_2 = \{z : z = z_1 + z_2, z_1 \in U_1, z_2 \in U_2\}$.

THEOREM 2.1. *The pseudospectra of A_W satisfy*

$$(2.7) \quad \Lambda(A_W) + \Delta_\epsilon \subseteq \Lambda_\epsilon(A_W) \subseteq \Lambda(A_W) + \Delta_{\kappa\epsilon} \quad \forall \epsilon \geq 0,$$

where κ is the condition number of the basis $\{\phi_j\}$. Equivalently, we have

$$(2.8) \quad \frac{1}{\text{dist}\{z, \Lambda(A_W)\}} \leq \|(zI - A_W)^{-1}\| \leq \frac{\kappa}{\text{dist}\{z, \Lambda(A_W)\}} \quad \forall z \in \rho(A_W).$$

The lower bound states that the ϵ -pseudospectrum of A_W contains the union of the closed ϵ -balls centered at the eigenvalues and is the trivial bound mentioned above. The upper bound is an extension of the Bauer–Fike theorem [11]; see Appendix B for an outline of the proof. If the eigenfunctions $\{\phi_j\}$ are orthonormal, then $\kappa = 1$. In this case, the upper and lower bounds are equal in both (2.7) and (2.8). This result verifies the characterization of a normal operator mentioned above. If $\kappa \gg 1$, then the theorem implies that the ϵ -pseudospectra may be much larger than the spectrum.

We now turn our attention to the numerical range (or field of values) of an operator. This set, which we denote by $\mathcal{F}(A)$, is defined for arbitrary linear operators [19].

DEFINITION. Let A be a linear operator. The numerical range of A is defined by

$$(2.9) \quad \mathcal{F}(A) = \{z : z = (Au, u), \text{ where } u \in D(A), \|u\| = 1\}.$$

The numerical range is a convex set. If A is a matrix, then its domain is the whole space, so the restriction $u \in D(A)$ is superfluous.

Like pseudospectra, the numerical range of a matrix can be computed in a straightforward manner. For the 2-norm, $\sup \operatorname{Re}(Au, u)$ and $\inf \operatorname{Re}(Au, u)$ are given by the largest and smallest eigenvalues of $(A + A^*)/2$, the *Hermitian part* of A , where $*$ denotes the Hermitian conjugate. Other points on the boundary of $\mathcal{F}(A)$ can be determined by considering the Hermitian parts of the rotated matrices $e^{i\theta} A$ for $\theta \in [0, \pi]$ [16]. For operators, bounds on the numerical range can be obtained, and the analysis often involves integration by parts; see §§4 and 6.

The pseudospectra and numerical range of an operator can be related. We must first make a technical assumption [19]. Let $\Sigma(A) = \mathbf{C} \setminus \overline{\text{cl}\{\mathcal{F}(A)\}}$. We assume that

(I) $\Sigma(A)$ is connected and $\Sigma(A) \cap \rho(A) \neq \emptyset$.

The first part of (I) requires that the set $\Sigma(A)$ consist of only one component (or piece). The second part requires that $\Sigma(A)$ not be contained in the spectrum of A . The O–S operator and the model operator satisfy (I); see §§4 and 6. With this assumption, we have the following result.

THEOREM 2.2. *Let A be a closed linear operator satisfying (I). The pseudospectra of A satisfy*

$$(2.10) \quad \Lambda_\epsilon(A) \subseteq \text{cl}\{\mathcal{F}(A)\} + \Delta_\epsilon \quad \forall \epsilon \geq 0.$$

Equivalently, we have

$$(2.11) \quad \|(zI - A)^{-1}\| \leq \frac{1}{\text{dist}\{z, \mathcal{F}(A)\}} \quad \forall z \notin \text{cl}\{\mathcal{F}(A)\}.$$

The proof of (2.11) is given in [19]. The theorem states that the ϵ -pseudospectrum lies within a distance ϵ of the numerical range. If we set $\epsilon = 0$, then (2.10) states that the spectrum of A lies in the closure of the numerical range.

In general, the sets Λ_ϵ contain more information about an operator than the single set \mathcal{F} . On the other hand, the computation of the numerical range is more amenable to analytic methods. We will find it useful to examine both the pseudospectra and the numerical range in our study of the O-S operator.

3. The Hille–Yosida theorem. A principal application of pseudospectra and the numerical range is the analysis of growth. Assume that A is closed, satisfies (I), and has a domain that is densely defined in \mathcal{H} . Consider the initial value problem

$$(3.1) \quad \frac{du}{dt} = -iAu, \quad u(0) = u_0,$$

where $u_0 \in \mathcal{H}$. This problem has a unique solution if the numerical range lies in a half-plane $\{z : \operatorname{Im} z \leq c\}$ for some fixed c [25]. This last condition ensures that a solution to (3.1) is bounded for any fixed $t \geq 0$.

The solution to (3.1) can be written as

$$(3.2) \quad u(t) = T(t)u_0,$$

where $T(t)$ is the semigroup generated by A . If A is a matrix, then, as is well known from the theory of ordinary differential equations, the solution is $u(t) = e^{-iAt}u_0$, where the matrix exponential can be defined via a Taylor series. To simplify the notation, we write $T(t) \equiv e^{-iAt}$ for all linear operators A .

There is no growth if $\|u(t)\| \leq \|u_0\|$ for all $t \geq 0$ and all initial conditions $u_0 \in \mathcal{H}$. Equivalently, there is no growth if the operator exponential satisfies

$$(3.3) \quad \|e^{-iAt}\| \leq 1 \quad \forall t \geq 0.$$

The standard condition requiring that $\Lambda(A)$ lie in the lower half-plane is necessary but not sufficient for (3.3) unless the operator A is normal. Necessary and sufficient conditions for (3.3) can be expressed in terms of the pseudospectra and the numerical range. Roughly speaking, *there is no growth if and only if the pseudospectra lie sufficiently close to the lower half-plane*. To measure this distance, we define

$$(3.4) \quad \beta_\epsilon = \sup_{z \in \Lambda_\epsilon(A)} \operatorname{Im} z.$$

The following theorem, which is a restatement of the Hille–Yosida theorem, is the main result on growth.

THEOREM 3.1. *Suppose that the linear operator A is closed, satisfies (I), and has domain $D(A)$ that is densely defined in \mathcal{H} . Then $\|e^{-iAt}\| \leq 1$ for all $t \geq 0$ if and only if any of the following equivalent conditions is satisfied:*

- (i) $\beta_\epsilon \leq \epsilon$ for all $\epsilon \geq 0$;
- (ii) $\|(zI - A)^{-1}\| \leq 1/\operatorname{Im} z$ for all z such that $\operatorname{Im} z > 0$;
- (iii) $\mathcal{F}(A)$ lies in the closed lower half-plane.

Condition (ii) is the standard condition for no growth [25], and (i) is the restatement of this condition in the language of pseudospectra. The sufficiency of (iii) follows from (ii) and Theorem (2.2). It can be shown that (iii) is necessary by showing that (ii) implies (iii); we omit the details.

Condition (iii) can also be shown to be necessary and sufficient by relating it to the so-called energy methods. These methods, which are valid for both linear and nonlinear problems [18], derive conditions for no growth by considering the evolution equation for $\|\phi\|^2 = (\phi, \phi)$. If ϕ is a solution to (3.1), then we formally have

$$(3.5) \quad \frac{d\|\phi\|^2}{dt} = (\phi, \frac{d\phi}{dt}) + (\frac{d\phi}{dt}, \phi) = (\phi, -iA\phi) + (-iA\phi, \phi) = 2\text{Im}(A\phi, \phi).$$

Here we have used the facts that $(\phi, \psi) = (\psi, \phi)^*$ and $(-i\phi, \psi) = -i(\phi, \psi)$. The rate of change of the energy ($\|\phi\|^2$) is nonpositive if and only if the numerical range of A lies in the closed lower half-plane.

The sharpest result for bounds on transient growth depends on powers of the resolvent and cannot be expressed in terms of the pseudospectra alone. The result is shown below [25].

THEOREM 3.2. *Suppose that the linear operator A is closed, satisfies (I), and has domain $D(A)$ that is densely defined in \mathcal{H} . Then $\|e^{-iAt}\| \leq C$ for all $t \geq 0$ if and only if*

$$(3.6) \quad \|(zI - A)^{-k}\| \leq \frac{C}{(\text{Im } z)^k} \quad \forall z \text{ satisfying } \text{Im } z > 0$$

and all integers $k > 0$.

A lower bound for growth can be expressed in terms of the pseudospectra. Let us define

$$(3.7) \quad C' = \sup_{\epsilon > 0} \frac{\beta_\epsilon}{\epsilon}.$$

The quantity C' is a measure of the extension of the pseudospectra into the upper half-plane. The relationship between pseudospectra and resolvents implies that

$$(3.8) \quad C' = \sup_{\text{Im } z > 0} (\text{Im } z) \|(zI - A)^{-1}\|.$$

Now, it can be shown that $C' \geq 1$ [19]. If $C' = 1$, then there is no growth by the Hille–Yosida theorem. For $C' > 1$, we obtain the result

$$(3.9) \quad C' > 1 \implies \sup_{t \geq 0} \|e^{-iAt}\| \geq C'.$$

This result follows from the fact that $C' \leq C$.

An upper bound for transient growth based on the pseudospectra can be derived using a resolvent integral; see §7.

4. Numerical range of the O–S operator. Before presenting results on the numerical range, we first discuss relevant properties of the O–S operator. The theoretical results described in the first part of this section were proved by DiPrima and Habetler [8].

The domain of the O–S operator is³

$$(4.1) \quad D(\mathcal{S}) = \left\{ \phi : \frac{d^3\phi}{dy^3} \text{ absolutely continuous, } \frac{d^4\phi}{dy^4} \in L^2[-1, 1], \phi(\pm 1) = \frac{d\phi}{dy}(\pm 1) = 0 \right\}.$$

³ See [19] for a definition of absolute continuity.

The domain of \mathcal{B} is

$$(4.2) \quad D(\mathcal{B}) = \left\{ \phi : \frac{d\phi}{dy} \text{ absolutely continuous, } \frac{d^2\phi}{dy^2} \in L^2[-1, 1], \phi(\pm 1) = 0 \right\}.$$

This last definition ensures that \mathcal{B} is invertible for all real wavenumbers α . From our definition in the Introduction, it follows that $\mathcal{S} : D(\mathcal{S}) \rightarrow D(\mathcal{B})$.

The norms of interest to us are the standard L^2 norm and the *energy norm*, which we denote by $\|\cdot\|_L$ and $\|\cdot\|_H$, respectively. For $\phi, \psi \in D(\mathcal{B})$, the energy norm of ϕ is defined by $\|\phi\|_H^2 = (\phi, \phi)_H$, where

$$(4.3) \quad (\phi, \psi)_H = (\mathcal{B}\phi, \psi)_L = - \int_{-1}^1 \psi^* \left(\frac{\partial^2 \phi}{\partial y^2} - \alpha^2 \phi \right) dy.$$

Here $(\cdot, \cdot)_L$ is the inner product associated with the L^2 norm. Integration by parts applied to the right-hand side of (4.3) implies that

$$(4.4) \quad \|\phi\|_H^2 = \int_{-1}^1 \left(\left| \frac{\partial \phi}{\partial y} \right|^2 + \alpha^2 |\phi|^2 \right) dy.$$

The energy norm is important for physical reasons because $\|\phi(\cdot, t)\|_H^2$ is proportional to the energy of the perturbation defined by the streamfunction $\Psi(x, y, t) = \phi(y, t)e^{i\alpha x}$.

The energy norm is important for theoretical purposes as well. Any function $f \in D(\mathcal{B})$ can be expanded in a convergent infinite series involving the generalized eigenfunctions $\{\phi_j\}$ of \mathcal{S} . The expansion coefficients of f can be computed by taking the energy norm inner product of f with the eigenfunctions of the adjoint O–S operator [29]. The appropriate underlying Hilbert space is $\mathcal{H} = D(\mathcal{B})$. In this space, the operator \mathcal{S} is closed and $D(\mathcal{S})$ is dense.

The completeness property of the O–S eigenfunctions implies that the solution to (1.3) can be written in terms of an eigenfunction expansion. Assuming that the eigenvalues are distinct, we have

$$(4.5) \quad \check{\phi}(y, t) = \sum_{j=1}^{\infty} a_j e^{-i\alpha\lambda_j t} \phi_j,$$

where the numbers $\{a_j\}$ are the expansion coefficients of $\phi(y, 0)$. This formula must be modified when there are degenerate eigenvalues [14]. We find (4.5) useful when we analyze transient growth in §7.

To determine the numerical range of \mathcal{S} , we examine the inner product

$$(4.6) \quad (\mathcal{S}\phi, \phi)_H = (\mathcal{B}\mathcal{S}\phi, \phi)_L = (\mathcal{A}\phi, \phi)_L, \quad \phi \in D(\mathcal{S}).$$

The simplifications in (4.6) follow from the definitions of the norm and \mathcal{S} . Using the expression for $\mathcal{A}\phi$, we have

$$(4.7) \quad \begin{aligned} (\mathcal{A}\phi, \phi)_L &= \frac{1}{i\alpha R} \int_{-1}^1 (\phi^* \phi^{(iv)} - 2\alpha^2 \phi^* \phi'' + \alpha^4 |\phi|^2) dy \\ &\quad - \int_{-1}^1 U(\phi^* \phi'' - \alpha^2 |\phi|^2) dy + \int_{-1}^1 U'' |\phi|^2 dy. \end{aligned}$$

Here, ' denotes differentiation with respect to y . After integrating the first and second terms by parts and using the fact that ϕ satisfies the two homogeneous conditions at each boundary, we find that the real and imaginary parts of the above expression satisfy

$$(4.8) \quad \xi = \operatorname{Re}(\mathcal{A}\phi, \phi)_L = \int_{-1}^1 (U|\phi'|^2 + \alpha^2 U|\phi|^2 + U''|\phi|^2) dy + \operatorname{Re} \int_{-1}^1 U'\phi^*\phi' dy$$

and

$$(4.9) \quad \eta = \operatorname{Im}(\mathcal{A}\phi, \phi)_L = -\frac{1}{\alpha R} \int_{-1}^1 (|\phi''|^2 + 2\alpha^2|\phi'|^2 + \alpha^4|\phi|^2) dy + \operatorname{Im} \int_{-1}^1 U'\phi^*\phi' dy.$$

Using the condition $\|\phi\|_H = 1$, it follows that ξ is bounded. The first term in (4.9) is negative. The second term may be positive, but it is bounded in magnitude. Noting these properties, let us define

$$(4.10) \quad \xi_{\min}(\alpha, R) = \inf_{\substack{\phi \in D(\mathcal{S}) \\ \|\phi\|_H = 1}} \xi, \quad \xi_{\max}(\alpha, R) = \sup_{\substack{\phi \in D(\mathcal{S}) \\ \|\phi\|_H = 1}} \xi,$$

and

$$(4.11) \quad \eta_{\max}(\alpha, R) = \sup_{\substack{\phi \in D(\mathcal{S}) \\ \|\phi\|_H = 1}} \eta.$$

We have proved the following result.

THEOREM 4.1. *The numerical range of the Orr-Sommerfeld operator satisfies*

$$(4.12) \quad \mathcal{F}(\mathcal{S}) \subseteq \{z : \xi_{\min}(\alpha, R) \leq \operatorname{Re} z \leq \xi_{\max}(\alpha, R), \operatorname{Im} z \leq \eta_{\max}(\alpha, R)\}.$$

The numerical range lies in a semi-infinite strip, and this ensures that $\Sigma(\mathcal{S})$ consists of one piece. Also, since $\Lambda(\mathcal{S})$ consists of discrete points and Σ is not the entire complex plane, it follows that the second part of (I) is satisfied as well. Hence, by Theorem 2.2, the spectrum of \mathcal{S} also lies in the strip defined by (4.12).

The functions ξ_{\min} , ξ_{\max} , and η_{\max} have been examined previously, but exact analytic expressions have not been derived. Joseph's general results [17], [9] yield the following bounds for Poiseuille flow:

$$(4.13) \quad -\frac{4}{\pi^2 + 4\alpha^2} \leq \xi \leq 1$$

and

$$(4.14) \quad \eta \leq \frac{1}{\alpha} - \frac{1}{\alpha R} \left\{ \frac{\pi^2(\pi^2 + \alpha^2)}{\pi^2 + 4\alpha^2} + \alpha^2 \right\}.$$

A more involved analysis shows that there is no growth if [17], [9]

$$(4.15) \quad R \leq \frac{1}{2\alpha} \max\{p^2\pi + 2^{3/2}\alpha^3, p^2\pi + \alpha^2\pi\},$$

where $p \approx 2.36$.

The critical Reynolds number for no growth can be characterized exactly by carefully examining the curve $\eta_{\max} = 0$. If we define $R_1(\alpha)$ to be the smallest value

of R such that $\eta_{\max} \geq 0$, then this function can be characterized as the solution of a constrained minimization problem [31]. By deriving the equivalent Euler equations, it can be shown that $R_1(\alpha)$ is the smallest eigenvalue λ of the problem

$$(4.16) \quad \phi^{(iv)} - 2\alpha^2 \phi'' + \alpha^4 \phi + i\alpha\lambda(U'\phi' + \frac{1}{2}U''\phi) = 0, \quad \phi(\pm 1) = \phi'(\pm 1) = 0.$$

Orr derived (4.16) using energy methods [23], [9] and showed that, if $R < R_g \equiv \min_\alpha R_1(\alpha) \approx 87.7$, then the energy of a two-dimensional perturbation to the mean Poiseuille flow does not grow. (For three-dimensional perturbations, the corresponding Reynolds number is ≈ 49.6 [18].) Note that (4.15) gives a lower bound for $R_1(\alpha)$. We will compute $R_1(\alpha)$ numerically in §7.

The above numerical range argument has an interesting history. It was first given by Synge to establish bounds on the eigenvalues and a condition for linear stability [31]. The starting point for the analysis is the O-S equation $\mathcal{A}\phi = \lambda\mathcal{B}\phi$, where λ is the eigenvalue. Multiplying by ϕ^* and integrating, we obtain $(\mathcal{A}\phi, \phi)_L = \lambda(\mathcal{B}\phi, \phi)_L$. If we assume that $\|\phi\|_H = 1$, then $(\mathcal{A}\phi, \phi)_L = \lambda$. The left-hand side of this equation is precisely the same as (4.6). It follows that the condition $\eta_{\max} \leq 0$ implies linear stability. As described above, $\eta_{\max} \leq 0$ actually implies that the numerical range of \mathcal{S} lies in the lower half-plane. We would like to stress that the condition that the numerical range lies in the lower half-plane is *much stronger* than the condition that the eigenvalues lie in the lower half-plane. By the Hille–Yosida theorem, the existence of growth can be deduced by examining the numerical range. On the other hand, *unless an operator is normal, linear stability alone does not give information about the existence of growth*. Now, Synge connected the linear stability result with Orr's equation (4.16) and discussed the fact that $\eta_{\max} \leq 0$ actually implies no growth. However, this connection is not always clearly explained when Synge's derivation is repeated; often, the connection is not mentioned at all.

5. Pseudospectra of the O–S operator. We now turn our attention to the pseudospectra of the O–S operator. We estimate the pseudospectra of the O–S operator by computing the pseudospectra of its discrete matrix analogues. We use a Chebyshev hybrid spectral discretization based on a method developed by Herbert [15]. The method combines an expansion in Chebyshev polynomials and collocation at the Chebyshev points with explicit enforcement of the boundary conditions. We check our results using the Chebyshev tau discretization, which was used by Orszag in his numerical studies of the O–S eigenvalues [24]. Both of these methods solve for the Chebyshev coefficients and convert the O–S operator \mathcal{S} to a matrix $\hat{\mathcal{S}}$ of dimension N .

The above-mentioned matrix $\hat{\mathcal{S}}$ is a representation of the *discrete O–S operator*, which we denote by S . Let P_{N-1} denote the space of polynomials of degree $N-1$. If $\phi \in P_{N-1}$ is a perturbation, then $\psi = S\phi$ is the discrete time derivative of this perturbation. The matrix $\hat{\mathcal{S}}$ is a particular representation of the discrete O–S operator and maps the Chebyshev coefficients of ϕ to the coefficients of ψ .

We compute the pseudospectra and the numerical range of the discrete O–S operator in the energy norm, and this is accomplished by introducing a weight matrix F . If $\phi \in P_{N-1}$ and u is the N -vector of its Chebyshev coefficients, then F is defined so that $\|\phi\|_H = \|Fu\|_2$, where the energy norm is defined by (4.4) and the subscript 2 refers to the discrete 2-norm. It can be shown that the resolvent norm satisfies the

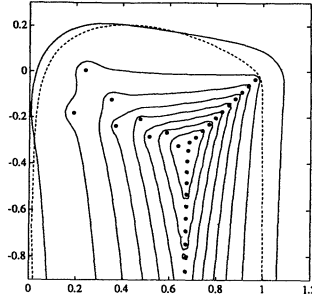


FIG. 2. *Pseudospectra and numerical range of the discretization operator S for $R = 10,000$ and $\alpha = 1$. The dashed curve is the boundary of the numerical range. The solid curves correspond to the boundaries of $\Delta_\epsilon(S)$ for $\epsilon = 10^{-8}, 10^{-7}, \dots, 10^{-1}$ and the dots are the eigenvalues of S . Here S is computed using the hybrid discretization with $N = 64$ modes.*

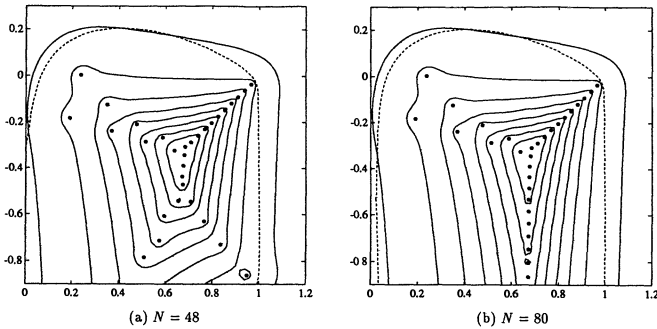


FIG. 3. *Same as Fig. 2. Here N modes are used in the discretization.*

formula⁴

$$(5.1) \quad \|(zI - S)^{-1}\|_H = \|F(zI - \hat{S})^{-1}F^{-1}\|_2.$$

See Appendix A for a proof of (5.1) and for the formulas for the elements of F . For the numerical range, we have

$$(5.2) \quad (S\phi, \phi)_H = u^* F \hat{S} F^{-1} u,$$

where u^* is the Hermitian conjugate of the vector of Chebyshev coefficients u . Using (5.2), it can be shown that the numerical range of S computed using the energy norm inner product is the same as the numerical range of the matrix $F \hat{S} F^{-1}$ computed using the 2-norm inner product.

Let us begin with a computation for $R = 10,000$. Here and throughout this section, we assume that $\alpha = 1$ and consider discretizations of the even part of the O-S operator only. Results for the odd part of the O-S operator are qualitatively similar. We use the hybrid discretization with $N = 64$ even modes. Figure 2 shows the

⁴ The domain of S is $D(S) = P_{N-1}$. An arbitrary function $\phi \in D(S)$ need not satisfy the homogeneous boundary conditions at $\phi(\pm 1) = \phi'(\pm 1) = 0$. Hence, $D(S)$ is not a subset of $D(\bar{S})$. It is possible to define a new discrete O-S operator \bar{S} such that $D(\bar{S}) \subseteq D(S)$ by projecting S onto the appropriate space; see Appendix B. For the results presented in this section, we find that $\|(zI - S)^{-1}\|_H$ and $\|(zI - \bar{S})^{-1}\|_H$ differ by less than one part in 10^3 .

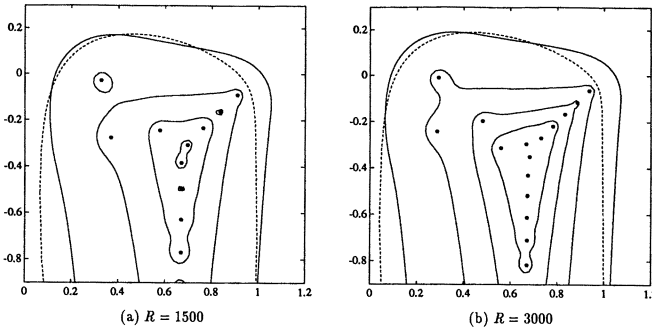


FIG. 4. Same as Fig. 2. The contours correspond to $\epsilon = 10^{-4}, \dots, 10^{-1}$.

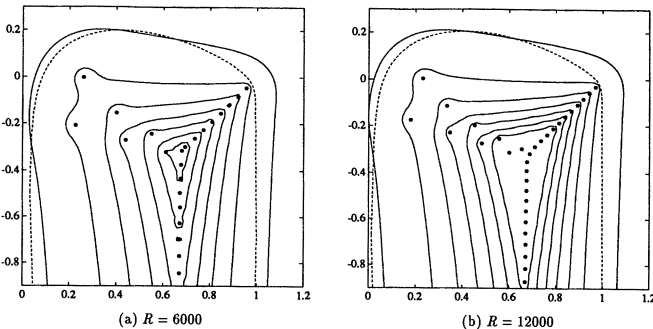


FIG. 5. Same as Fig. 2. The contours correspond to $\epsilon = 10^{-7}, \dots, 10^{-1}$.

boundaries of the pseudospectra (solid lines) and the numerical range (dashed line). This plot reveals several fundamental properties of the discrete O–S operator. First, S is far from normal; if this operator were normal, then the ϵ -pseudospectra would lie within a distance ϵ of the spectrum. Second, the eigenvalues at the intersection of the branches are the most sensitive to perturbations. We examine this point in more detail in this and the following sections. Third, the high sensitivity of the eigenvalues at the intersection is not revealed by the numerical range. Hence, although analysis of the numerical range is appropriate for studying growth, it does not yield detailed information about the eigenvalues lying inside the numerical range. Finally, note that the numerical range of the discrete O–S operator satisfies the bounds (4.13) and (4.14), derived for the continuous O–S operator. We see that the ϵ -pseudospectra lie within a distance ϵ of the numerical range; in this plot, only $\Lambda_\epsilon(\mathcal{S})$ for $\epsilon = 0.1$ extends outside $\mathcal{F}(\mathcal{S})$.

Figure 2 was produced by computing the resolvent norm on a 60×60 grid in the z -plane. We find that the resolvent norm $\|(zI - S)^{-1}\|_H$ changes by less than 2 percent at these gridpoints if S is rederived using the tau discretization with $N = 64$ even modes. The pseudospectra of S do depend on the number of modes N , and this is illustrated in Fig. 3. Note that $N = 48$ modes are not sufficient to resolve the modes below the intersection of the branches. On the other hand, the boundaries of the pseudospectra of S for $N = 64$ and $N = 80$ are indistinguishable; we find that the relative difference in $\|(zI - S)^{-1}\|_H$ is ≈ 1 percent.

The dependence of the pseudospectra on the Reynolds number is shown in Figs. 4 and 5. Here we use the hybrid discretization with $N = 64$ even modes. The size

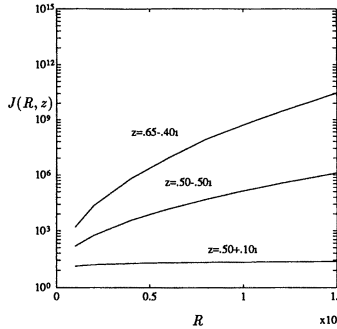


FIG. 6. Dependence of $\|(zI - S)^{-1}\|_H$ on the Reynolds number and the point z .

of $\Lambda_\epsilon(S)$ for $\epsilon \ll 1$ at the intersection of the branches increases dramatically with R . For example, compare the ϵ -pseudospectrum for $\epsilon = 10^{-4}$ in Fig. 4 and the ϵ -pseudospectrum for $\epsilon = 10^{-7}$ in Fig. 5. Note that the numerical range does not change significantly as R is increased.

The dependence of the pseudospectra on R can be examined quantitatively by measuring the norm of the resolvent at various points. We consider (a) $z = .65 - .4i$, (b) $z = 0.5 - .5i$, and (c) $z = 0.5 + .1i$. These points may lie in the numerical range of S . Point (a) lies at the intersection of the branches, (b) lies slightly away from the intersection, and (c) lies in the upper half-plane.

The dependence of $J(R, z) = \|(zI - S)^{-1}\|_H$ on the Reynolds number is plotted in Fig. 6. This function grows dramatically with R if z is near the intersection of the branches. Based on our results for the model problem presented in the next section, we conjecture that, if z is near the intersection of the branches, then the controlling factor in the behavior of $J(R, z)$ is $e^{a_z R^\gamma}$ for some $\gamma < 1$.⁵ For point (c), $J(R, z)$ grows by only a factor of 2 when R increased from 1,000 to 15,000. If $\operatorname{Re} z > 1$, $\operatorname{Re} z < -4/\pi^2$, or if $\operatorname{Im} z > 1/\alpha$, then, by (4.13), (4.14), and Theorem 2, z lies outside the numerical range for all R and $J(R, z)$ is bounded independent of R .

It is also instructive to examine the condition number of the O-S eigenfunction basis. Let W be the space spanned by the eigenfunctions $\{\phi_j\}$ of S associated with the K eigenvalues $\{\lambda_j\}$ satisfying $\lambda_j > -.9$ and let κ denote the condition number of this basis. A detailed explanation of how to compute κ is given in Appendix B. We choose this value of K for two reasons. First, these eigenvalues and eigenfunctions are good estimates of the corresponding eigenvalues and eigenfunctions of the actual O-S operator. Therefore, we expect that our computed κ is a good approximation to the condition number of the eigenfunction basis of the corresponding subspace of $D(S)$. Second, this choice includes the modes at the intersection of the branches. As we showed above, the eigenvalues at the intersection of the branches are highly sensitive to perturbations. This implies that the associated eigenfunctions are nearly linearly independent. As our plots suggest, the eigenvalues further below the real axis are not as sensitive to perturbations as those at the intersection. This implies that the associated eigenfunctions are nearly orthogonal to the space W and that the condition number of the eigenfunction basis for the enlarged space is not significantly

⁵ For the model problem, we show that $\gamma = .5$. Fitting $J(R, z)$ to the exponential function with this value of γ gives the values $a_z \approx .19$ and $\approx .1$ for the points (a) and (b), respectively.

TABLE 1

Condition number of the eigenfunction basis of the space W . The space W is spanned by the K eigenfunctions of S associated to the eigenvalues with maximal imaginary part.

R	K	κ
1,000	9	2.57×10^2
2,000	13	6.29×10^3
4,000	19	1.01×10^5
6,000	23	2.47×10^6
8,000	27	2.03×10^7
10,000	30	1.59×10^8
12,000	33	8.87×10^8
15,000	37	1.54×10^{10}

greater than κ .

Table 1 lists κ as a function of R . As mentioned in §2, κ is a rough upper bound for the magnitude of the expansion coefficients of a function of norm 1. The results in this table show that expansions in the eigenfunctions may involve large coefficients when the Reynolds number is large. Roughly speaking, we find that $\kappa \sim e^{\gamma R^{1/2}}$. This relation implies that a quadrupling of R leads to a squaring of the condition number. Hence, the expansion coefficients may be as large as $\approx 10^{16}$ if $R \approx 40,000$ (and $\alpha = 1$). At this Reynolds number, eigenfunction expansions may be affected by rounding errors in double precision arithmetic (16 digits). For Cray double precision (32 digits), the corresponding Reynolds number is $\approx 160,000$.

The condition number and the resolvent norm depend on the choice of the norm. We have presented results for the energy norm because it can be interpreted physically; it is related to the actual energy of perturbations. We find that the results are qualitatively similar if the L^2 norm is used. On the other hand, it is possible to choose an inner product such that the O-S eigenfunctions are orthogonal. However, the new norm generated by this inner product may not be physically relevant.

We find that the results for the odd part of the O-S operator for Poiseuille flow and the O-S operator for Couette flow are qualitatively similar to the results presented here. For the odd part of the O-S operator, κ and $J(R, z)$ at the three points are of the same order of magnitude as in the even case. For Couette flow, we find that the condition number of the eigenfunction basis of a space similar to W is $O(10^6)$ for $R = 1,000$. The reason why this condition number is much greater than that for Poiseuille flow for the same R is not known.

Previously, theoretical work had been done on the resolvent of operators arising in hydrodynamic stability. For example, Yudovich considered the Navier-Stokes operator for a bounded three-dimensional domain [35]. He estimated the resolvent in the upper half-plane using Green's functions and other theoretical techniques and then used the estimates to bound the growth of initial perturbations. While these estimates give bounds for the growth, they do not give a complete picture of the properties of the operator. As our computations suggest, the resolvent norm may grow only weakly as a function of R for points in the upper half-plane. This does not reflect the behavior of the resolvent near the intersection of the branches or the behavior of the condition number of the eigenfunction basis.

We have presented results on the pseudospectra and numerical range of the discrete O-S operator. The fundamental question is the following: Do the pseudospectra and the numerical range of the discrete analogues approximate the pseudospectra and the numerical range of the O-S operator? There has been much work on the rela-

tionship between the eigenvalues and eigenvectors of an operator and those of its spectral and finite difference analogues [6]. The relationship between the pseudospectra and numerical range of an operator to those of its discrete analogues is not as well understood.

There are two main reasons why the pseudospectra of the O–S operator may differ from the pseudospectra of its discrete analogue. First, discretization operators have finite resolution. If the number of modes is not sufficient, then the discretization scheme is not able to resolve features of eigenfunctions, and this leads to poor approximations of both the eigenvalues and eigenfunctions of the operator. This phenomenon is illustrated in Fig. 3(a). The pseudospectra of an operator and its discrete analogue also differ if there are too few modes to resolve the pseudo-eigenfunctions. Suppose that z is not an eigenvalue of \mathcal{S} . There is a normalized function $u_z \in D(\mathcal{S})$ such that $\|(\mathcal{S} - zI)u_z\|$ is minimized or nearly minimized over all normalized functions $u \in D(\mathcal{S})$. Roughly speaking, $\|(zI - \mathcal{S})^{-1}\|$ is close to $\|(zI - \mathcal{S})^{-1}\|$ if u_z can be resolved; see [26] for examples of this phenomenon. The effect of finite resolution on the pseudospectra becomes less significant as the number of modes is increased.

Second, the pseudospectra of a discrete analogue are affected by parasitic modes. Our discrete O–S operator S has two artificial eigenvalues due to the manner in which the boundary conditions are implemented. These eigenvalues can be moved to an arbitrary position, and we have put them at $z = -200i$, far away from the intersection of the branches.

Although these differences exist, we find that the pseudospectra of the discrete O–S operator are independent of the discretization and that the sensitivity of the eigenvalues at the intersection of the branches and the condition number of the eigenfunction basis increase exponentially with the Reynolds number. We believe that these properties of the discrete O–S operator are a reflection of the properties of the O–S operator.

6. Pseudospectra of a model differential operator. To gain some insight into why the pseudospectra of the O–S operator behave as they do, we consider the model operator

$$(6.1) \quad \mathcal{T} = -\frac{1}{i\alpha R} \frac{d^2}{dy^2} + y.$$

The domain of \mathcal{T} can be chosen as the set of functions $\phi \in L^2[-1, 1]$ having an absolutely continuous first derivative, a second derivative in $L^2[-1, 1]$, and satisfying the boundary conditions $\phi(\pm 1) = 0$. The associated eigenvalue problem is

$$(6.2) \quad \frac{1}{i\alpha R} \frac{d^2\phi}{dy^2} - (y - \lambda)\phi = 0$$

with boundary conditions

$$(6.3) \quad \phi(-1) = \phi(1) = 0,$$

where λ is the eigenvalue. Except for a constant factor, which simply translates the spectrum and the pseudospectra, \mathcal{T} is the same as the homogeneous operator governing the normal vorticity for three-dimensional perturbations to Couette flow [7], [13]. The eigenvalue problem can also be related to the O–S equation for plane Couette flow via an order reduction [9]. Without loss of generality, we assume that $\alpha = 1$.

It is convenient to choose the underlying Hilbert space to be $L^2[-1, 1]$. The operator \mathcal{T} is closed in this space, and $D(\mathcal{T})$ is dense [19].

We first turn our attention to the spectrum of \mathcal{T} . It can be shown that $\Lambda(\mathcal{T})$ is Y -shaped, consists of a countable number of points, and is symmetric about the imaginary axis.⁶ If we assume that $|\lambda|$ is large, then the y term in (6.2) can be neglected, and it can be shown that the eigenvalues $\{\lambda_n\}$ of \mathcal{T} satisfy

$$(6.4) \quad \lambda_n \approx -\frac{in^2\pi^2}{4R} \quad \text{as } n \rightarrow \infty.$$

Asymptotic estimates of the eigenvalues in the two upper branches for large R can also be derived using techniques developed for approximating the O-S eigenvalues [29].

It is straightforward to bound the numerical range of \mathcal{T} . Choosing $\phi \in D(\mathcal{T})$, we have

$$(6.5) \quad \begin{aligned} (\mathcal{T}\phi, \phi)_L &= -\frac{1}{iR} \int_{-1}^1 \phi^* \phi'' dy + \int_{-1}^1 y |\phi|^2 dy \\ &= -\frac{i}{R} \int_{-1}^1 |\phi'|^2 dy + \int_{-1}^1 y |\phi|^2 dy, \end{aligned}$$

where again we have integrated by parts. The first term is imaginary. The second term is real and is bounded by 1 in absolute value since $\|\phi\|_L = 1$. Hence, we have proved the following theorem.

THEOREM 6.1. *The numerical range of \mathcal{T} satisfies*

$$(6.6) \quad \mathcal{F}(\mathcal{T}) \subseteq \{z : |\operatorname{Re} z| \leq 1, \operatorname{Im} z \leq 0\}$$

for all $R > 0$.

The theorem states that the numerical range of \mathcal{T} lies in a strip that lies in the lower half-plane for all $R > 0$. This last result and the fact that $\Lambda(\mathcal{T})$ consists of a discrete set of points implies that \mathcal{T} satisfies (I). Hence, by the Hille-Yosida theorem, Theorem 6.1 implies the following growth result: If $\phi(y, t)$ is a solution to the differential equation

$$(6.7) \quad \frac{\partial \phi}{\partial t} = -\frac{1}{iR} \frac{\partial^2 \phi}{\partial y^2} + y\phi, \quad \phi(\pm 1, t) = 0, \quad \phi(y, 0) = \phi_0,$$

where $R > 0$, then $\|\phi(\cdot, t)\|_L \leq \|\phi_0\|_L$ for all $t \geq 0$ and all $\phi_0 \in L^2[-1, 1]$.

In [7] a calculation similar to the one above is used to show that the eigenvalues of the homogeneous normal vorticity equation lie in the lower half-plane. Again, the calculation actually shows that the numerical range lies in the lower half-plane.

Before considering \mathcal{T} , let us briefly examine the pseudospectra of a discrete version of \mathcal{T} . This operator can be approximated by one of the methods described in §5. The discretization converts \mathcal{T} into a matrix $\hat{\mathcal{T}}$. Figure 7(a) shows the 35 eigenvalues of $\hat{\mathcal{T}}$ for $R = 1,500$ with maximal imaginary part and an approximation to its ϵ -pseudospectrum for $\epsilon = 10^{-6}$ via random perturbations. Figure 7(b) shows similar results for $R = 3,000$. These results show that the eigenvalues at the intersection of the branches are highly sensitive to perturbations and that the sensitivity increases dramatically with R .

⁶ If λ is not an eigenvalue of \mathcal{T} , then the resolvent $(\lambda I - \mathcal{T})^{-1}$ is a compact operator, and this implies that the spectrum of \mathcal{T} is countable [19, §III.6.7]. If $\phi(y) = \phi_1(y) + i\phi_2(y)$ is an eigenfunction with eigenvalue $\lambda = a + ib$, where a, b, ϕ_1 , and ϕ_2 are real, then $\tilde{\phi}(y) = \phi_1(-y) - i\phi_2(-y)$ is an eigenfunction with eigenvalue $\tilde{\lambda} = -a + ib$.

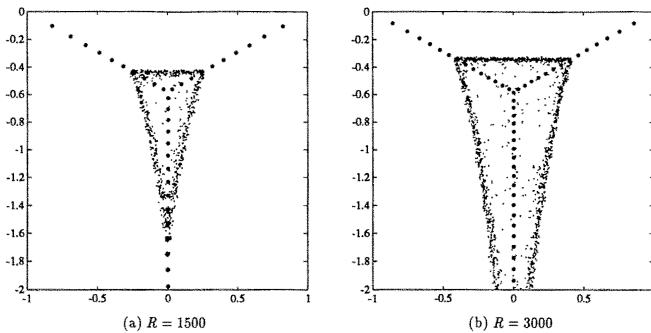


FIG. 7. The spectrum and approximate ϵ -pseudospectrum for $\epsilon = 10^{-6}$ of the matrix \hat{T} , defined here by a Chebyshev tau approximation with $N = 128$ modes. The large dots are the eigenvalues of \hat{T} with maximal imaginary part. The small dots are the eigenvalues of 50 randomly perturbed matrices $\hat{T} + E$, where $\|E\|_2 = 10^{-6}$.

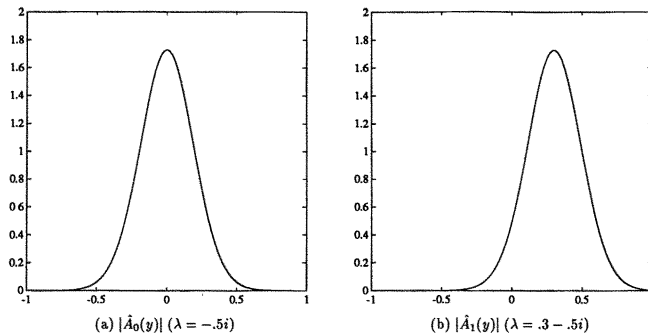


FIG. 8. Plots of the functions $|\hat{A}_0|$ and $|\hat{A}_1|$ for $\lambda = -.5$ and $\lambda = .3 - .5i$, respectively, with $R = 1,500$.

Now we turn our attention to the operator \mathcal{T} itself. The differential equation (6.2) can be solved analytically. Let $\gamma = (iR)^{1/3}$ and $w = \gamma(y - \lambda)$. Then (6.2) can be transformed into the Airy equation

$$(6.8) \quad \frac{d^2\phi}{dw^2} - w\phi = 0.$$

As is well known, any solution of (6.8) can be written as a linear combination of any two of the three Airy functions $A_0(y) = Ai(w)$, $A_1(y) = Ai(\beta w)$, and $A_2(y) = Ai(\beta^2 w)$, where $\beta = e^{i2\pi/3}$. Let $\hat{A}_j(y) = A_j(y)/\|A_j(y)\|_L$, $j = 1, 2, 3$ denote the normalized Airy functions. The functions $|\hat{A}_0|$ and $|\hat{A}_1|$ are plotted in Fig. 8 for $\lambda = -5i$ and $\lambda = .3 - .5i$, respectively.⁷

Figure 7(a) shows that $\lambda = -.5i$ is not an eigenvalue of \mathcal{T} . On the other hand, the normalized function \hat{A}_0 is a solution to the differential equation (6.2), and Fig. 8(a) shows that this function nearly satisfies the boundary conditions ($|\hat{A}_0(\pm 1)| \approx 10^{-4}$). Though $\lambda = -.5i$ is not an eigenvalue, the existence of such a solution to (6.2) implies that λ lies in the ϵ -pseudospectrum for $\epsilon = O(10^{-4})$. The proof is straightforward. Suppose that ϕ is a normalized solution to the differential equation and satisfies

⁷ We evaluate $Ai(w)$ for complex w using the routines described in [2].

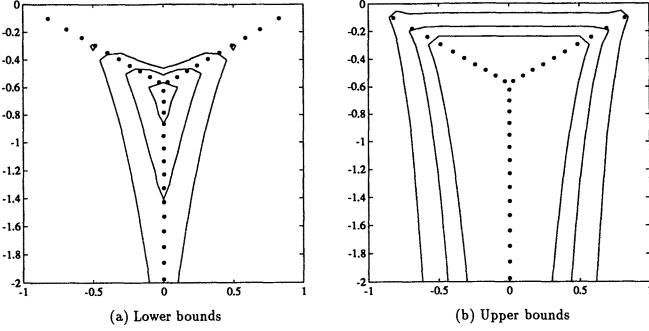


FIG. 9. Lower and upper bounds for the pseudospectra of \mathcal{T} for $R = 1,500$. The solid dots are the eigenvalues of \mathcal{T} . The contours in (a) and (b) are the lower and upper bounds of the ϵ -pseudospectra for $\epsilon = 10^{-2}, 10^{-3}$, and 10^{-4} .

$|\phi(\pm 1)| \approx \delta \ll 1$. The function ϕ is not a pseudo-eigenfunction since it does not satisfy the boundary conditions. However, let us define

$$(6.9) \quad u = \phi(y) + \xi(y),$$

where ξ is a smooth function satisfying $\|\xi\|_L = O(\delta)$, chosen so that $u \in D(\mathcal{T})$. For example, ξ can be chosen as the unique function of the form $\xi = c_1 y + c_2$, where c_1 and c_2 are constants. Then

$$(6.10) \quad \frac{\|(\mathcal{T} - \lambda I)u\|_L}{\|u\|_L} = \frac{\|(\mathcal{T} - \lambda I)\xi\|_L}{\|u\|_L} = O(\delta),$$

since $\|u\|_L \approx \|\phi\|_L = 1$. This implies that $\|(\mathcal{T} - \lambda I)^{-1}\|_L$ is bounded below by $O(\delta^{-1})$, and hence $\lambda \in \Lambda_\epsilon(\mathcal{T})$ for $\epsilon = O(\delta)$. This argument can be generalized to show that if there is a solution to the O-S equation (1.5) that satisfies the boundary conditions to within a factor of δ , then λ lies in the ϵ -pseudospectrum of the O-S operator for $\epsilon = O(\delta)$.

The above analysis shows that $\lambda = -.5i$ and $\lambda = .3 - .5i$ lie in the ϵ -pseudospectrum for $\epsilon \ll 1$. It follows that the eigenvalues at the intersection of the branches are highly sensitive to perturbations since these points lie a distance ≈ 0.1 from $\Lambda(\mathcal{T})$. See Fig. 7. If \mathcal{T} were normal, then a number $\lambda \in \Lambda_\epsilon(\mathcal{T})$ would lie within a distance ϵ of the spectrum of \mathcal{T} .

The above method allows us to use (2.3) to compute a lower bound for the pseudospectra. For each λ , we choose the pseudo-eigenfunction to be $u = \hat{A}_j + \xi$, where ξ is the unique affine function mentioned above and \hat{A}_j is one of the three Airy functions, chosen so that $\|(\mathcal{T} - \lambda I)u\|_L/\|u\|_L$ is minimized. For example, the functions \hat{A}_0 and \hat{A}_1 are chosen for $\lambda = -.5i$ and $\lambda = .3 - .5i$, respectively. In the cases where this lower bound is poorer than that predicted by the trivial bound (2.2), we choose the latter. The lower bounds for the pseudospectra of \mathcal{T} for $R = 1,500$ and $R = 3,000$ are plotted in Figs. 9(a) and 10(a).

An upper bound for the pseudospectra can be determined by computing an upper bound for the resolvent, and this can be accomplished using the Green's function $C(y, s, \lambda)$ for (6.2), (6.3). This is a standard technique for bounding the resolvent [19], [35]. Consider the inhomogeneous problem $(\mathcal{T} - \lambda I)\phi = -f$ with the boundary

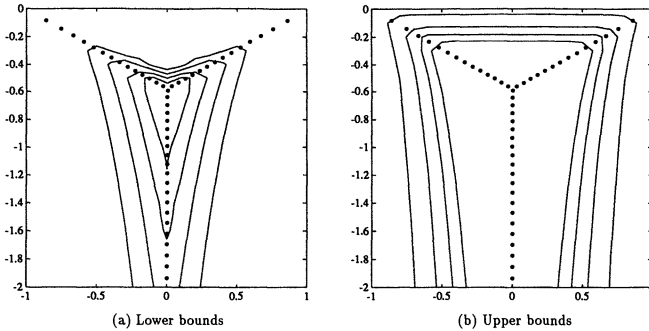


FIG. 10. Same as Fig. 9 for $R = 3,000$. The contours correspond to $\epsilon = 10^{-2}, 10^{-3}, \dots, 10^{-5}$.

conditions (6.3), where $f \in L^2[-1, 1]$. The solution is

$$(6.11) \quad \phi(y) = (\lambda I - T)^{-1}f = \int_{-1}^1 C(y, s, \lambda)f(s)ds.$$

Applying the Cauchy-Schwartz inequality to (6.11) twice, we obtain the bound [19, p. 144]

$$(6.12) \quad \|(\lambda I - T)^{-1}\|_L^2 \leq \int_{-1}^1 \int_{-1}^1 |C(y, s, \lambda)|^2 ds dy.$$

The Green's function can be expressed in the form

$$(6.13) \quad \begin{aligned} C(y, s, \lambda) &= \frac{iRv_1(y)v_2(s)}{W(s)} & -1 \leq y \leq s \leq 1 \\ &= \frac{iRv_2(y)v_1(s)}{W(s)} & -1 \leq s \leq y \leq 1, \end{aligned}$$

where v_1 and v_2 are solutions to (6.2) that satisfy $v_1(-1) = 0$ and $v_2(1) = 0$, respectively, and where W is the Wronskian of these two functions [19, §III.2.3].

We estimate the integral (6.12) using routines from QUADPACK. The functions v_1 and v_2 are defined in terms of a linear combination of the two of the three functions \hat{A}_j that are the least linearly dependent. The Wronskian of any two solutions of (6.2) is a constant, which can be determined using the known values of the pairwise Wronskians for the functions $Ai(w)$, $Ai(\beta w)$, and $Ai(\beta^2 w)$ [1]. The computed upper bounds for the pseudospectra of T for $R = 1,500$ and $R = 3,000$ are plotted in Figs. 9(b) and 10(b).

The lower and upper bounds for the ϵ -pseudospectra in the figures show that the eigenvalues at the intersection of the branches are highly sensitive to perturbations and that the sensitivity increases with R . There is a qualitative agreement between the upper and lower bounds, but the quantitative agreement is not good, especially for $\epsilon \ll 1$. It might be possible to improve the lower bound by choosing the function ϕ differently.

Using the above procedure for computing a lower bound, we can show that $\|(\lambda I - T)^{-1}\|_L$ depends exponentially on R for values of λ near the intersection of the branches. Consider the resolvent for $\lambda = -i$ as the parameter R is increased. The following calculations neglect all algebraic factors in R . The graph of \hat{A}_0 for

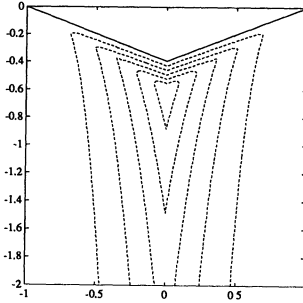


FIG. 11. *Contours of a_λ . The solid line corresponds to $a_\lambda = 0$. The dashed curves correspond to $a_\lambda = .05, .1, \dots, .25$.*

$\lambda = -i$ has the same bell curve shape as the graph of \hat{A}_0 for $\lambda = -.5i$ shown in Fig. 8. Therefore $|A_0(0)| \approx \|A_0\|_L$ except for an algebraic factor. The controlling factor in the asymptotic expansion of the Airy function is

$$(6.14) \quad Ai(w) \approx \exp\left(-\frac{2}{3}w^{3/2}\right) \quad \text{as } w \rightarrow \infty.$$

Since $A_0(y) = Ai(w)$, where $w = (iR)^{1/3}(y + i)$, we obtain

$$(6.15) \quad |A_0(0)| \approx \exp\left(\frac{2}{3}R^{1/2}\right) \quad \text{as } R \rightarrow \infty$$

and

$$(6.16) \quad |A_0(\pm 1)| \approx \exp\left(\frac{2^{7/4}}{3}R^{1/2} \cos \frac{5\pi}{8}\right) \quad \text{as } R \rightarrow \infty.$$

Hence the magnitude of the normalized function $\hat{A}_0(y)$ at the boundaries is given by

$$(6.17) \quad |\hat{A}_0(\pm 1)| \approx \exp(-.24R^{1/2}) \quad \text{as } R \rightarrow \infty.$$

It follows that $\|(\lambda I - T)^{-1}\|_L$ increases exponentially with R . We do not claim that the estimate (6.17) is sharp.

This approach can be used to estimate the asymptotic behavior of the lower bound for the resolvent $b(\lambda)$. If $-1 < \operatorname{Re} \lambda < 1$ and λ is sufficiently far below the real axis, then the controlling factor of this function is

$$(6.18) \quad b(\lambda) \approx e^{a_\lambda R^{1/2}} \quad \text{as } R \rightarrow \infty,$$

where a_λ is a parameter depending on the point λ . The contours of a_λ are plotted in Fig. 11. This figure shows that the resolvent grows exponentially with R if $-1 < \operatorname{Re} \lambda < 1$ and λ lies below the solid line. On the other hand, if $|\operatorname{Re} \lambda| > 1$ or $\operatorname{Im} \lambda > 0$, then, by Theorems 2.2 and 6.1, $\|(\lambda I - T)^{-1}\|_L$ is bounded independent of R . More careful analysis is required to determine the precise behavior of $\|(\lambda I - T)^{-1}\|_L$ for λ in the triangular region above the solid line in Fig. 11, but we do not pursue that here.

Our results show that the sensitivity of the eigenvalues of the model operator near the intersection of the branches is related qualitatively to the existence of solutions

to the associated differential equation that satisfy the boundary conditions to within an exponentially small factor. We believe that this mechanism is responsible for the sensitivity of the eigenvalues of the O–S operator as well. We have not proved that the existence of such solutions is necessary for highly sensitive eigenvalues. On the other hand, in previous work, it has been found that this feature is common to other classes of operators that have highly sensitive eigenvalues, including Toeplitz matrices [28], constant-coefficient differential operators, and Wiener–Hopf integral operators [3], [26]. In each case, the resolvent behaves exponentially with respect to some parameter in some critical region of the complex plane. Outside the critical region, the resolvent is uniformly bounded with respect to the parameter.

7. Transient energy growth. The energy of a two-dimensional perturbation to plane Poiseuille flow does not grow if the Reynolds number is less than $R_g \approx 87.7$. On the other hand, if $R > R_c \approx 5772$, then the flow may be linearly unstable, and there is the potential for unbounded growth in the energy of a perturbation. If $R_g < R < R_c$, then the energy of a perturbation decays to zero as $t \rightarrow \infty$. However, there may be growth in the energy before the decay. In this section, we examine transient growth for plane Poiseuille flow.

Let us assume that $R_g < R < R_c$. If the initial perturbation $\phi(y, 0) = \phi_0(y)$ is precisely an eigenfunction of \mathcal{S} , then it decays exponentially in norm. Instead, let us suppose that ϕ_0 is a superposition of the K eigenfunctions $\{\phi_j\}$ associated with the eigenvalues $\{\lambda_j\}$ with maximal imaginary part. Let W denote the space spanned by these eigenfunctions and let \mathcal{S}_W denote the projection of the full O–S operator onto this space. The operator \mathcal{S}_W is finite-dimensional and maps a perturbation in W to its time derivative. If $\phi_0 \in W$, then the evolution of this perturbation can be written as

$$(7.1) \quad \phi(y, t) = e^{-i\alpha\mathcal{S}_W t} \phi_0(y);$$

see §3. The energy growth is defined by

$$(7.2) \quad G(t) = \sup_{\phi_0 \in W} \frac{\|\phi(\cdot, t)\|_H^2}{\|\phi_0\|_H^2} = \|e^{-i\alpha\mathcal{S}_W t}\|_H^2.$$

We have included the square in (7.2) because the energy of a perturbation is proportional to the square of the energy norm. Finally, let us define $G_{\max} = \sup_{t \geq 0} G(t)$ to be the maximum growth for all time.

The existence of growth when $R < R_c$ can be understood by writing (7.1) in terms of an eigenfunction expansion. We have

$$(7.3) \quad \phi(y, t) = \sum_{j=1}^K a_j e^{-i\alpha\lambda_j t} \phi_j(y),$$

where the numbers $\{a_j\}$ are the coefficients in the expansion of $\phi_0(y)$. Now, if the condition number of the eigenfunction basis is large, then some of the expansion coefficients of a perturbation with $\|\phi_0\|_H = 1$ may be large. At $t = 0$, the large terms cancel. Now, although $\|a_j e^{-i\alpha\lambda_j t} \phi_j\|_H$ decreases monotonically, it may still be large for values of $t > 0$ if a_j is large. In this case, the right-hand side of (7.3) is still a sum of large terms, but the cancellation that occurs for $t = 0$ need not occur for $t > 0$.

We compute $G(t)$ numerically. We first determine the eigenvalues and eigenfunctions using a spectral method. We then apply the procedure for projecting an operator

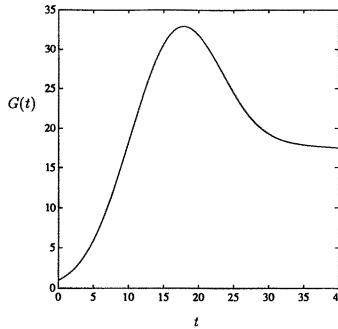


FIG. 12. Plot of the maximum growth in the energy as a function of time for $R = 5,000$ and $\alpha = 1$.

onto a space of eigenfunctions to produce a matrix S_W that is an approximation to S_W ; see Appendix B. We compute the matrix exponential using routines from Matlab. We find that a good approximation to $G(t)$ can be obtained if the sum (7.3) includes the terms satisfying $\text{Im } \lambda_j \geq - .9$. The key is to include the eigenvalues at the intersection of the branches. Including eigenvalues with $\text{Im } \lambda_j < - .9$ does not improve the result for two reasons. First, for these eigenvalues, $|e^{-i\alpha\lambda_j t}| \ll 1$ if $t > 0$. Second, if λ_j is well below the intersection, then the associated expansion coefficient a_j is moderate in size. This property is related to the fact that the associated eigenfunction ϕ_j is nearly orthogonal to the eigenfunctions at the intersection of the branches.

Figure 12 shows a plot $G(t)$ for $R = 5,000$ and $\alpha = 1$. The maximum growth is $G_{\max} \approx 32.9$. The transient phase corresponds to t less than ≈ 25 , and the large growth is due to the cancellation effects mentioned above. For $t \geq 25$, the function $G(t)$ is governed by the eigenvalues near the real axis; see Fig. 14. If the O-S operator were normal, then there would be no transient phase, and the function $G(t)$ would decay from the outset.

For each $t \geq 0$, there is an initial condition $\phi_0 \in W$ with norm 1 such that $\|\phi(y, t)\|_H^2 = G(t)$. The initial condition depends on t and can be computed using the singular value decomposition of $e^{-i\alpha S_W t}$ [11]; see [10] for a description of the characteristics of the initial condition. We find that the largest of the coefficients $\{a_j\}$ of the initial condition that achieves the growth G_{\max} in our example is of magnitude $O(10^4)$ and that these large coefficients are associated with the modes at the intersection of the branches—that is, $\text{Im } \lambda_j \approx - .3$. For the eigenvalue with $\text{Im } \lambda_j \approx - .9$, we have $|a_j| \approx O(10^{-2})$.

Growth for plane Poiseuille flow at subcritical Reynolds numbers has been studied previously. Shantini examined the possibility of growth due to degenerate eigenvalues of the O-S operator at special values of α and R [30]. She found no growth from the O-S degeneracies alone using the generalized eigenfunction as an initial condition. We would like to emphasize that *degenerate eigenvalues are not necessary for growth*. Growth at subcritical Reynolds numbers is due to the nonnormality of the O-S operator. An operator with a degenerate eigenvalue is nonnormal. However, a nonnormal operator need not have degenerate eigenvalues. *In general, the function $G(t)$ can only be determined by computing the norm of the operator exponential (7.2).*

Our procedure for computing growth is essentially the same as that used by Farrell [10], who investigated transient growth for Poiseuille and Couette flows. However, there are two important differences. First, we use spectral methods instead of finite

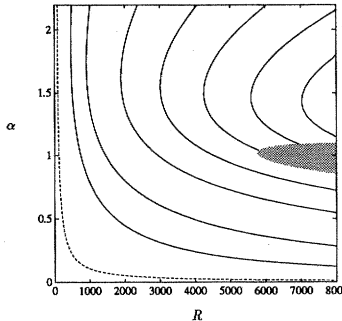


FIG. 13. Level curves of G_{\max} . The shaded region corresponds to the region where the O-S operator is linearly unstable. This implies that $G_{\max} = \infty$. The dashed line is the critical curve $R_1(\alpha)$ and corresponds to $G_{\max} = 1$. The solid lines, from left to right, are the level curves for $G_{\max} = 5, 10, 20, 30, 40, 50, 60$.

differences to compute the eigenvalues and eigenvectors. Second, by recognizing that the modes far below the intersection of the branches do not contribute significantly to $G(t)$, we attempt to use as few modes K as possible. This can lead to substantial savings in computational work, since the norm calculation in (7.2) requires $O(K^3)$ operations. Finally, we mention that both methods may be affected by rounding errors at high Reynolds numbers, since they make explicit use of the eigenvalues and eigenfunctions in an intermediate calculation; see §5. In this section, this difficulty does not arise because the calculations involve relatively low Reynolds numbers.

The method for computing the growth can be used to determine the maximum growth G_{\max} as a function of R and α . If S has an eigenvalue in the upper half-plane, then $G_{\max} = \infty$. If $R \leq R_1(\alpha)$, where $R_1(\alpha)$ is the critical Reynolds number for no growth defined by (4.16), then $G_{\max} = 1$. Now, if the flow is linearly stable and $R > R_1(\alpha)$, then $1 < G_{\max} < \infty$, and we can compute the maximum growth. We can determine $R_1(\alpha)$ using the spectral discretization procedure described in §5.

The level curves of G_{\max} are shown in Fig. 13. We see that there can be significant energy growth, even if the flow is linearly stable. For $\alpha = 1.45$ and $R = 5772$, we find that $G_{\max} \approx 51$. The critical value $R_1(\alpha)$ is minimized when $\alpha \approx 2.1$, and we find that $R_g \approx 87.6$. A lower bound for $R_1(\alpha)$ for the limits $\alpha \rightarrow 0$ and $\alpha \rightarrow \infty$ is given by (4.15). If the O-S operator were normal for all R and α , then the dashed line would coincide with the boundary of the shaded region, and there would not be a transient growth region in the figure.

It is instructive to examine the effects of small perturbations on G_{\max} . As the contours of the resolvent in Fig. 14 suggest, the eigenvalues of S_W near the intersection of the branches are highly sensitive to perturbations. Now, although perturbations have a significant effect on some of the eigenvalues, they have *relatively little effect on the maximum transient growth*. To see this, we define $\tilde{G}(t) = \|e^{-i\alpha(S_W+E)t}\|_H^2$ and $\tilde{G}_{\max} = \sup_{t \geq 0} \tilde{G}(t)$, where E is a random matrix satisfying $\|E\|_H = 10^{-5}$. We find that \tilde{G}_{\max} differs from G_{\max} by $\approx 8 \times 10^{-5}$, even though some eigenvalues have shifted by a distance ≈ 0.1 . For $t \leq 40$, the absolute difference between the functions $\tilde{G}(t)$ and $G(t)$ is less than 8×10^{-3} .

This example illustrates a fundamental point about nonnormal operators: Although the eigenvalues of a nonnormal operator can be highly sensitive to perturbations, the behavior of the operator in applications may be insensitive to perturbations.

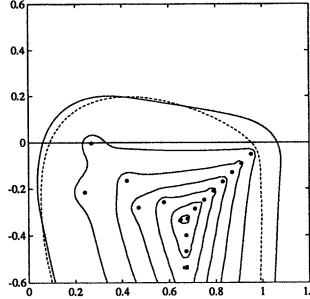


FIG. 14. Pseudospectra and numerical range of the operator S_W for $R = 5,000$ and $\alpha = 1$. The dashed line is the boundary of the numerical range. The solid contours are the boundaries of the $\Lambda_\epsilon(S_W)$ for $\epsilon = 10^{-1}, 10^{-2}, \dots, 10^{-7}$. The dots are the eigenvalues of S_W .

Another such application is the norm; elementary properties of the norm imply that if $\|E\|_H = \epsilon$, then $\|S_W + E\|_H$ differs from $\|S_W\|_H$ by at most ϵ .

We end this section by showing how the results on growth in §3 can be applied to our example. Figure 14 shows the pseudospectra and numerical range of S_W . The numerical range extends into the upper half-plane, and this immediately shows that there is growth. A rough lower bound for the growth can be determined by considering the $\epsilon = .1$ contour. We see that $\beta_\epsilon \approx .2$, and therefore $\beta_\epsilon/\epsilon \approx 2$. By Theorem 3.2, it follows that $\sup_{t \geq 0} \|e^{-i\alpha S_W t}\|_H \geq 2$. As shown in §3, a sharper lower bound for the growth is given by the quantity $C' = \sup_{\text{Im } z > 0} \text{Im } z \| (zI - S_W)^{-1} \|_H$. This quantity can be determined by searching for the supremum in the upper half of the z -plane. We find that $C' = 3.6$.

An upper bound for the growth can be determined using the resolvent integral

$$(7.4) \quad e^{-i\alpha S_W t} = \frac{1}{2\pi i} \int_{\Gamma} e^{-i\alpha zt} (zI - S_W)^{-1} dz.$$

Here Γ is a contour enclosing the spectrum of S_W [19, §I.5.6]. A convenient contour is the square with corners at $z = 0$, $z = 1$, $z = 1 - i$, and $z = -i$. On this contour, we have

$$(7.5) \quad 2\pi \|e^{-i\alpha S_W t}\| = \left\| \int_{\Gamma} e^{-i\alpha zt} (zI - S_W)^{-1} dz \right\|_H \leq \int_{\Gamma} \|(zI - S_W)^{-1}\|_H |dz|.$$

The value of this last integral is 19.2. This bound can be improved by choosing the contour Γ more carefully. Hence, we have

$$(7.6) \quad 3.6 \leq \sup_{t \geq 0} \|e^{-i\alpha S_W t}\|_H \leq 19.2.$$

The actual value of the supremum in (7.6) is $\sqrt{32.9} \approx 5.7$.

The techniques used to bound $e^{-i\alpha S_W t}$ can also be used to bound the matrix exponential of the full O-S operator \mathcal{S} . Let $t_1 > 0$ be arbitrary. For $t \geq t_1$, we can compute an upper bound for the growth using a resolvent integral. In this case, we choose Γ to be the infinite rectangle with corners at $c_1 - i\infty$, c_1 , c_2 , and $c_2 - i\infty$. We choose c_1 and c_2 so that the numerical range lies within the infinite sides of the rectangle. By Theorem 2.2, this choice ensures that $\|(zI - \mathcal{S})^{-1}\|$ is bounded independent of z on the contour and that the resolvent integral converges. For $0 \leq t \leq t_1$, we can bound the growth using a more general version of the Hille-Yosida theorem [25]. See also [35] for various growth results based on resolvent estimates.

8. Conclusion. The Orr–Sommerfeld operator is nonnormal—that is, it does not have a complete set of orthogonal eigenfunctions. The behavior of a normal operator in most applications is governed by its spectrum. The eigenvalues of a nonnormal operator A may be highly sensitive to perturbations. It is more appropriate to analyze the behavior of a nonnormal operator using the ϵ -pseudospectra and the numerical range. For nonnormal operators, these sets may be much larger than the spectrum.

In this paper, we analyze the pseudospectra and the numerical range of the O–S operator for Poiseuille flow. We obtain bounds on the numerical range using integration by parts, and we compute the pseudospectra by means of discrete analogues and a model problem. We find that the pseudospectra are much larger than the spectrum. In particular, the eigenvalues at the intersection of the \mathbf{A} , \mathbf{P} , and \mathbf{S} branches are highly sensitive to perturbations and the associated eigenfunctions are nearly linearly dependent. The sensitivity and the condition number of the eigenfunction basis increase exponentially with the Reynolds number. Our analysis of the model problem suggests that this phenomenon can be qualitatively explained by the existence of solutions to the eigenvalue equation that satisfy the boundary conditions to within an exponentially small factor.

These results have several important theoretical and practical implications. First, expansions in the O–S eigenfunctions can involve huge coefficients. This effect becomes exponentially more pronounced as the Reynolds number increases. If $R \approx O(40,000)$, then the magnitude of the coefficients can be as large as (10^{16}) , and expansions using double-precision arithmetic may be affected by rounding errors.

The nonnormality of the O–S operator also implies that there may be growth of initial perturbations when all the eigenmodes decay exponentially. Eigenvalue analysis predicts the correct long-term behavior but cannot be used to check for transient growth. There is no transient growth if and only if the numerical range of the O–S operator lies in the lower half-plane, and this condition is equivalent to that obtained by energy methods.

For plane Poiseuille flow, we find growth by a factor as large as ≈ 51 at subcritical Reynolds numbers before the asymptotic decay predicted by the eigenvalues sets in. Similar results were previously found by Farrell for plane Poiseuille and Couette flows [10]. The transient growth at subcritical Reynolds numbers may be understood as follows: If a normalized initial perturbation is a superposition of nearly linearly dependent eigenfunctions, then its expansion coefficients will be large. The large terms in the expansion cancel each other out to give an initial condition of order 1. Since each eigenmode evolves independently, the cancellations that occur initially need not continue to occur thus leading to transient growth. The initial conditions that yield the maximum growth can be determined from the matrix exponential of the O–S operator.

The effects of nonnormality of the governing operator become more prominent in the stability analysis of three-dimensional perturbations. The linearized three-dimensional operator consists of the O–S operator coupled with an operator that governs the evolution of the normal vorticity. By computing the matrix exponential, Butler and Farrell show that there may be growth in the energy by a factor as large as $O(1,000)$ at subcritical Reynolds numbers [4] for Poiseuille flow. Growth for three-dimensional perturbations has been noted by previous researchers; see Shantini [30], Gustavsson [12], and Henningson and Schmid [14], among others. They examine growth resulting from degeneracies of the two-dimensional O–S eigenvalues and reso-

nance and near resonance between O-S and normal vorticity modes. These methods do not choose the optimal initial perturbations, and the growth found is lower than that found by Butler and Farrell.

The sensitivity of the O-S eigenvalues has been noted in previous numerical studies. The sensitivity was not attributed to the properties of the O-S operator but instead usually associated with the numerical discretization. In recent work, Kerner reported difficulties in numerically computing the eigenvalues of the Alfvén waves operator, which arises in magnetohydrodynamics [20]. The spectrum of this operator also consists of three branches. He finds that the eigenvalues at the intersection of the branches cannot be computed accurately when the resistivity is small. His plots show that the associated eigenfunctions decay exponentially at the boundaries. These facts suggest that the reason for the computational difficulties is the nonnormality of the operator and not insufficient numerical resolution.

Nonnormal operators arise in many fields. Examples include Toeplitz matrices, constant-coefficient differential operators, and Wiener-Hopf integral operators. We emphasize that qualitative information about the pseudospectra of an operator can easily be obtained by considering the pseudospectra of its discrete matrix analogues. A few eigenvalue calculations involving the perturbed discrete matrix or calculations of its resolvent can give information about the sensitivity of the eigenvalues, the applicability of eigenfunction expansions, and the potential for transient growth.

Appendix A. Weighted norms. Let v be an N -vector of Chebyshev coefficients. We define the polynomial associated to v by

$$(A.1) \quad \phi(y) = \sum_{j=0}^{N-1} v_j T_j(y),$$

where the coefficients v_j are the elements of the vector v and $T_j(y)$ is the j th Chebyshev polynomial.

The norms $\|\phi\|_L$ and $\|\phi\|_H$ can be computed directly from the Chebyshev coefficients. Let us first consider the L^2 norm. We have

$$(A.2) \quad \|\phi\|_L^2 = \int_{-1}^1 |\phi|^2 dy = \int_{-1}^1 \sum_{j=0}^{N-1} \sum_{k=0}^{N-1} v_j^* v_k T_j T_k dy.$$

Let M be the square matrix of dimension N defined by

$$(A.3) \quad M_{jk} = \int_{-1}^1 T_j T_k dy = \begin{cases} 0 & j + k \text{ odd}, \\ \frac{1}{1-(j+k)^2} + \frac{1}{1-(j-k)^2} & j + k \text{ even}, \end{cases}$$

where the indices satisfy $0 \leq j, k \leq N - 1$. It follows that

$$(A.4) \quad \|\phi\|_L^2 = \sum_{j=0}^{N-1} \sum_{k=0}^{N-1} v_j^* M_{jk} v_k = v^* M v.$$

The matrix M is symmetric, and therefore it can be decomposed in the form $M = E^* E$. This implies that

$$(A.5) \quad \|\phi\|_L = \sqrt{v^* E^* E v} = \|Ev\|_2.$$

Hence the L^2 norm of ϕ is equivalent to the weighted 2-norm of its Chebyshev coefficients. The energy norm of ϕ can be expressed in a similar manner using the weight matrix F defined by

$$(A.6) \quad \|\phi\|_H^2 = \int_{-1}^1 (|\phi'|^2 + \alpha^2 |\phi|)^{1/2} dy = \|Fv\|_2^2.$$

Here $F^*F = D_1^*MD_1 + \alpha^2 M$, where D_1 is the first derivative matrix, which maps the Chebyshev coefficients of $\phi(y)$ to the Chebyshev coefficients of $\phi'(y)$ [5].

Let P_{N-1} be the space of polynomials of degree $N - 1$ and suppose that $A : P_{N-1} \rightarrow P_{N-1}$ is an operator. The operator A can be represented by a matrix of dimension N . The matrix representation of A , which we denote by \hat{A} , depends on the choice of basis for the space P_{N-1} . Suppose that \hat{A} is defined in terms of the basis of Chebyshev polynomials and v is the N -vector of Chebyshev coefficients of ϕ . If $A\phi = \psi$, then $\hat{A}v = u$, where u is the vector of Chebyshev coefficients of ψ . The L^2 norm and the energy norm of A are obtained by a weighted norm of \hat{A} . For the energy norm, for example, (A.6) implies that

$$(A.7) \quad \|A\|_H = \sup_{\phi \neq 0} \frac{\|\psi\|_H}{\|\phi\|_H} = \sup_{v \neq 0} \frac{\|Fu\|_2}{\|Fv\|_2} = \sup_{v \neq 0} \frac{\|F\hat{A}v\|_2}{\|Fv\|_2}.$$

Substituting $w = Fv$ into the right-hand side of (A.7), we obtain

$$(A.8) \quad \|A\|_H = \sup_{w \neq 0} \frac{\|F\hat{A}F^{-1}w\|_2}{\|w\|_2} = \|F\hat{A}F^{-1}\|_2.$$

Hence, the energy norm of the operator A is equivalent to the 2-norm of $F\hat{A}F^{-1}$. Given the representation \hat{A} in the Chebyshev basis, it becomes a simple matter to compute $\|A\|_L$ and $\|A\|_H$, since the 2-norm of a matrix is readily evaluated using the singular value decomposition.

Appendix B. Projection of a matrix onto a space of eigenfunctions. Let $\{\phi_j\}$ be a set of K eigenfunctions of the discrete O–S operator S , with associated eigenvalues $\{\lambda_j\}$, and let W denote the space spanned by these eigenfunctions. If $\phi \in W$, then $\psi = S\phi$ also satisfies $\psi \in W$. The operator S can be projected onto the space W . This projected operator, which we denote by S_W , satisfies $S\phi = S_W\phi$ for all $\phi \in W$.

The operator S_W can be represented by a matrix of dimension K , which we denote by \hat{S}_W . The matrix representation depends on the basis chosen for W . If, for example, the basis is the set of eigenfunctions $\{\phi_j\}$, then $\hat{S}_W \equiv D_W$, where D_W is the matrix with the eigenvalues $\{\lambda_j\}$ on the diagonal. For reasons that become clear below, we define a matrix representation of S_W based on an orthonormal basis for W .

Let v_j be the vector of Chebyshev coefficients associated with ϕ_j and let V_W be the matrix of the vectors $\{v_j\}$. If we assume that $\|\phi_j\|_H = 1$, then $\|Fv_j\|_2 = 1$, where F is the energy norm weight matrix defined in Appendix A. We can compute an orthonormal basis $\{\psi_j\}$ for W by applying the QR decomposition [11] to the matrix FV_W . This is equivalent to applying the Gram–Schmidt procedure to the vectors $\{Fv_j\}$. We have

$$(B.1) \quad FV_W = (FQ_W)U_W.$$

The columns of Q_W satisfy $\|Fq_j\|_2 = 1$ and $q_j^* F^* F q_k = 0$ if $j \neq k$. Let ψ_j be the polynomial associated to q_j by a Chebyshev expansion. These polynomials satisfy $\|\psi_j\|_H = 1$ and $(\psi_j, \psi_k)_H = 0$ if $j \neq k$ and hence form an orthonormal basis for W . The matrix U_W is a square matrix of dimension K , which relates the expansion coefficients in the bases $\{\phi_j\}$ and $\{\psi_j\}$. If $p \in W$ and

$$(B.2) \quad p(y) = \sum_{j=1}^K a_j \phi_j(y) = \sum_{j=1}^K b_j \psi_j(y),$$

then $b = U_W a$, where a and b are the K -vectors of the expansion coefficients in (B.2). It is straightforward to check that

$$(B.3) \quad \|p\|_H = \|b\|_2.$$

Since D_W is the matrix representation of S_W in the eigenfunction basis and U_W relates that basis to the orthonormal basis, it follows that the matrix representation of S_W in the orthonormal basis is

$$(B.4) \quad \hat{S}_W = U_W D_W U_W^{-1}.$$

It follows from (B.3) that

$$(B.5) \quad \|S_W\|_H = \|\hat{S}_W\|_2$$

and

$$(B.6) \quad \|e^{-i\alpha S_W t}\|_H = \|e^{-i\alpha \hat{S}_W t}\|_2.$$

In addition, we have

$$(B.7) \quad \|(zI - S_W)^{-1}\|_H = \|(zI - \hat{S}_W)^{-1}\|_2 = \|U_W(zI - D_W)^{-1}U_W^{-1}\|_2,$$

where the last equality follows from (B.4). Since, D_W is diagonal, it follows that

$$(B.8) \quad \begin{aligned} \|(zI - S_W)^{-1}\|_H &\leq \|U_W\|_2 \|U_W^{-1}\|_2 \|(zI - D_W)^{-1}\|_2 \\ &= \frac{\kappa}{\text{dist}\{z, \Lambda(S_W)\}} \quad \forall z \notin \Lambda(S_W), \end{aligned}$$

where $\kappa = \|U_W\|_2 \|U_W^{-1}\|_2$ is the condition number.

Acknowledgments. We thank Nick Trefethen for his many contributions to this paper. In addition to constant encouragement during the course of this project, he made valuable comments on several early drafts of this paper and generously allowed us to use his Cray account and programs. We also thank Isom Herron and Håkan Gustavsson for their comments on the paper. Finally, we express our gratitude to Professor C. C. Lin for taking the time to discuss hydrodynamic stability with us.

REFERENCES

- [1] M. ABRAMOWITZ AND I. STEGUN, EDS., *Handbook of Mathematical Functions*, National Bureau of Standards, Washington, DC, 1964.
- [2] D. E. AMOS, *A portable package for Bessel functions of a complex argument and nonnegative order*, ACM Trans. Math. Software, 12 (1986), pp. 265–273.
- [3] P. M. ANSELONE AND I. H. SLOAN, *Spectral approximations for Wiener–Hopf operators*, J. Integral Equations Appl., 2 (1988), pp. 237–261.
- [4] K. M. BUTLER AND B. F. FARRELL, *Three-dimensional optimal perturbations in viscous shear flow*, Phys. Fluids A, 4 (1992), pp. 1637–1650.
- [5] C. CANUTO, M. Y. HUSSAINI, A. QUARTERONI, AND T. ZANG, *Spectral Methods in Fluid Dynamics*, Springer-Verlag, New York, 1988.
- [6] F. CHATELIN, *Spectral Approximation of Linear Operators*, Academic Press, New York, 1983.
- [7] A. DAVEY AND W. H. REID, *On the stability of stratified viscous plane Couette flow. Part 1. Constant buoyancy frequency*, J. Fluid Mech., 30 (1969), pp. 509–525.
- [8] R. C. DiPRIMA AND G. J. HABETLER, *A completeness theorem for non-selfadjoint eigenvalue problems in hydrodynamic stability*, Arch. Rat. Mech. Anal., 34 (1969), pp. 218–227.
- [9] P. G. DRAZIN AND W. H. REID, *Hydrodynamic Stability*, Cambridge University Press, Cambridge, UK, 1981.
- [10] B. F. FARRELL, *Optimal excitation of perturbations in viscous shear flow*, Phys. Fluids, 31 (1988), pp. 2093–2102.
- [11] G. H. GOLUB AND C. F. VAN LOAN, *Matrix Computations*, 2nd ed., Johns Hopkins University Press, Baltimore, MD, 1989.
- [12] L. H. GUSTAVSSON, *Energy growth of three-dimensional disturbances in plane Poiseuille flow*, J. Fluid Mech., 224 (1991), pp. 241–260.
- [13] L. H. GUSTAVSSON AND L. HULTGREN, *A resonance mechanism in plane Couette flow*, Stud. Appl. Math., 68 (1980), pp. 149–159.
- [14] D. S. HENNINGSON AND P. J. SCHMID, *Vector eigenfunction expansions of plane channel flows*, Stud. Appl. Math., 87 (1992), pp. 15–43.
- [15] T. HERBERT, *Die Neutrale Fläche der Ebenen Poiseuille-Strömung*, Habilitationsschrift, Univ. Stuttgart, Stuttgart, Germany, 1977.
- [16] A. S. HOUSEHOLDER, *The Theory of Matrices in Numerical Analysis*, Blaisdell, New York, 1965.
- [17] D. D. JOSEPH, *Eigenvalue bounds for the Orr–Sommerfeld equation, Part 2*, J. Fluid Mech., 36 (1969), pp. 721–734.
- [18] ———, *Stability of Fluid Motions I*, Springer-Verlag, Berlin, 1976.
- [19] T. KATO, *Perturbation Theory for Linear Operators*, Springer-Verlag, New York, 1976.
- [20] W. KERNER, *Large-scale complex eigenvalue problems*, J. Comput. Phys., 85 (1989), pp. 1–85.
- [21] L. M. MACK, *A numerical study of the temporal eigenvalue spectrum of the Blasius boundary layer*, J. Fluid Mech., 73 (1976), pp. 497–520.
- [22] N. M. NACHTIGAL, L. REICHEL, AND L. N. TREFETHEN, *A hybrid GMRES algorithm for nonsymmetric linear systems*, SIAM J. Matrix Anal. Appl., 13 (1992), pp. 796–825.
- [23] W. M. ORR, *The stability or instability of the steady motions of a perfect liquid and of a viscous liquid. Part II: A viscous liquid*, Proc. Roy. Irish Acad. A, 27 (1907), pp. 69–138.
- [24] S. A. ORSZAG, *Accurate solution of the Orr–Sommerfeld equation*, J. Fluid Mech., 50 (1971), pp. 689–703.
- [25] A. PAZY, *Semigroups of Linear Operators and Applications to Partial Differential Equations*, Springer-Verlag, New York, 1983.
- [26] S. C. REDDY, *Pseudospectra of Operators and Discretizations Matrices and an Application to Stability of the Method of Lines*, Ph.D. thesis, Massachusetts Institute of Technology, Cambridge, MA, 1991.
- [27] S. C. REDDY AND L. N. TREFETHEN, *Stability of the method of lines*, Numer. Math., 62 (1992), pp. 235–267.
- [28] L. REICHEL AND L. N. TREFETHEN, *The eigenvalues and pseudo-eigenvalues of Toeplitz matrices*, Linear Algebra Appl., 162 (1992), pp. 153–185.
- [29] I. V. SCHENSTED, *Contributions to the Theory of Hydrodynamic Stability*, Ph.D. thesis, Univ. of Michigan, Ann Arbor, MI, 1961.
- [30] R. SHANTINI, *Degenerating Orr–Sommerfeld eigenmodes and development of three-dimensional perturbations*, Ph.D. thesis, Univ. of Lulea, Sweden, 1990.
- [31] J. L. SYNGE, *Hydrodynamic stability*, Semicentenn. Publ. Amer. Math. Soc., 2 (1938), pp. 227–269.
- [32] L. N. TREFETHEN, *Nonnormal matrices and pseudospectra*, in preparation.

- [33] L. N. TREFETHEN, *Approximation theory and numerical linear algebra*, in Algorithms for Approximation II, J. Mason and M. Cox, eds., Chapman and Hall, London, 1990.
- [34] ———, *Pseudospectra of matrices*, in Numerical Analysis 1991, D. F. Griffiths and G. A. Watson, eds., Longman, White Plains, NY, 1992.
- [35] V. I. YUDOVICH, *The Linearization Method in Hydrodynamical Stability Theory*, American Mathematical Society, Providence, RI, 1989.